Available online at www.sciencedirect.com
ScienceDirect
Bioorganic & Medicinal Chemistry 15 (2007) 5018–5034
Bioorganic & Medicinal Chemistry

Structural basis for the activity of the RSK-specific inhibitor, SL0101

Jeffrey A. Smith,[a,b] David J. Maloney,[c] Sidney M. Hecht[c,d,*] and Deborah A. Lannigan[a,e,*]

[a]*Center for Cell Signaling, University of Virginia, Charlottesville, VA 22908, USA*
[b]*Department of Pathology, University of Virginia, Charlottesville, VA 22908, USA*
[c]*Department of Chemistry, University of Virginia, Charlottesville, VA 22904, USA*
[d]*Department of Biology, University of Virginia, Charlottesville, VA 22904, USA*
[e]*Department of Microbiology, University of Virginia, Charlottesville, VA 22908, USA*

Received 6 March 2007; revised 29 March 2007; accepted 29 March 2007
Available online 2 April 2007

Abstract—Inappropriate activity of p90 ribosomal S6 kinase (RSK) has been implicated in various human cancers as well as other pathologies. We previously reported the isolation, characterization, and synthesis of the natural product kaempferol 3-*O*-(3″,4″-di-*O*-acetyl-α-L-rhamnopyranoside), termed SL0101 [Smith, J. A.; Poteet-Smith, C. E.; Xu, Y.; Errington, T. M.; Hecht, S. M.; Lannigan, D. A. *Cancer Res.*, **2005**, *65*, 1027–1034: Xu, Y.-M; Smith, J. A.; Lannigan, D. A.; Hecht, S. M. *Bioorg. Med. Chem.*, **2006**, *14*, 3974–3977: Maloney, D. J.; Hecht, S. M. *Org. Lett.*, **2005**, *7*, 1097–1099]. SL0101 is a potent and specific inhibitor of RSK; therefore, we performed an analysis of the structural basis for the inhibitory activity of this lead compound. In in vitro kinase assays we found that acylation of the rhamnose moiety and the 4′, 5, and 7-hydroxyl groups are responsible for maintaining a high affinity interaction of RSK with SL0101. It is likely that the hydroxyl groups facilitate RSK binding through their ability to form hydrogen bonds. To determine whether the SL0101 derivatives were specific for inhibition of RSK we analyzed their ability to preferentially inhibit the growth of the human breast cancer line, MCF-7, compared to the normal human breast line, MCF-10A. We have previously validated this differential growth assay as a convenient readout for analyzing the specificity of RSK inhibitors [Smith, J. A.; Maloney, D. J.; Clark, D. E.; Xu, Y.-M.; Hecht, S. M.; Lannigan, D. A. *Bioorg. Med. Chem.*, **2006**, *14*, 6034–6042]. We found that acylation of the rhamnose moiety was essential for maintaining the selectivity for RSK inhibition in intact cells. Further, the efficacy of SL0101 in intact cells is limited by cellular uptake as well as possible hydrolysis of the acetyl groups on the rhamnose moiety by ubiquitous intracellular esterases. These studies should facilitate the development of a RSK inhibitor, based on the SL0101 pharmacophore, as an anti-cancer chemotherapeutic agent.

1. Introduction

The members of the p90 ribosomal S6 kinase family are downstream effectors of p42/p44 mitogen activated protein kinase (MAPK).[1] There is accumulating evidence that RSK plays a role in a number of different cancers.[2–6] These studies are partly based on our discovery of the RSK-specific inhibitor, SL0101 (kaempferol 3-*O*-(3″,4″-di-*O*-acetyl-α-L-rhamnopyranoside)) (**1**), which was initially isolated from an extract from *Forsteronia refracta*, a member of the Apocynaceae (dogbane) family found in the South American rainforest.[2,7] SL0101 (**1**) inhibits the proliferation of the human breast cancer cell line, MCF-7.[2] Remarkably, however, SL0101 (**1**) does not alter the growth of the normal human breast line MCF-10A, even though SL0101 (**1**) inhibits RSK activity in MCF-7 and MCF-10A cells.[2] Taken together, these results suggest that RSK may be an important new anti-cancer target.

Protein kinases have been shown to be excellent drug targets and a number of kinase inhibitors are being successfully used as anti-cancer agents in the clinic.[8] Protein kinases form a large superfamily of proteins that contain a conserved overall folding pattern for the kinase catalytic domain. The dual-lobed structure contains a smaller lobe for binding of Mg·ATP and a larger lobe for association with the substrate. Another conserved feature is an 'activation loop' near the catalytic center that differs in size and sequence among various kinases.

Keywords: Kaempferol 3-*O*-(3″,4″-di-*O*-acetyl-α-L-rhamnopyranoside); SL0101; RSK; Kinase inhibitor; Structure–activity relationship.
* Corresponding authors. Tel.: +1 434 924 3906; fax: +1 434 924 7856 (S.M.H.); tel.: +1 434 924 1144; fax: +1 434 924 1236 (D.A.L.); e-mail addresses: sidhecht@virginia.edu; dal5f@virginia.edu

0968-0896/$ - see front matter © 2007 Elsevier Ltd. All rights reserved.
doi:10.1016/j.bmc.2007.03.087

However, in spite of the high degree of similarity between the active sites of protein kinases there are now a number of examples of very specific inhibitors that utilize the ATP binding pocket and compete with ATP binding.[9] RSK is an unusual kinase in that it contains two non-identical functional kinase domains, an N-terminal kinase domain (NTKD) and a C-terminal kinase domain (CTKD).[1] The NTKD is responsible for phosphorylating exogenous substrates; the only known function of the CTKD is autophosphorylation. The natural product, SL0101 (**1**), is a kaempferol glycoside that belongs to the class of kinase inhibitors that are ATP competitors.[2] In vitro and cell-based assays have demonstrated that SL0101 (**1**) is potent and remarkably specific for inhibition of RSK NTKD activity.[2] Thus, SL0101 (**1**) is useful as a lead compound.

To further develop SL0101 (**1**) as an anti-cancer agent we analyzed the affinity and specificity of various SL0101 derivatives for inhibition of RSK activity. We have determined that acylation of the rhamnose moiety is essential for the specific inhibition of RSK activity, whereas the 4′, 5, and 7-hydroxyl groups on the kaempferol backbone of SL0101 are required for affinity. It is likely that the phenolic hydroxyl groups facilitate RSK binding by virtue of their ability to participate in hydrogen bonding. We have also found that increasing the hydrophobic character of SL0101 increases its potency of inhibition of RSK activity in cell-based assays, presumably by facilitating cellular uptake. Thus, this information should be helpful in designing the next generation of RSK inhibitors based on the SL0101 pharmacophore.

2. Results

2.1. The ATP binding pocket of the RSK NTKD is unique

Recently an atomic model of the RSK2 NTKD was described, which docks the distinct molecular scaffolds, SL0101, GF109203X, and the staurosporine derivative, Ro31-8820.[10] We compared this model to the X-ray crystal structures of the archetypal kinases, protein kinase A[11] and protein kinase C (PKC),[12] both of which were solved as complexes with staurosporine. We focused on those residues that comprise the ATP binding pocket for each kinase. Initially, we superimposed these structures and removed the amino acid residues contributed by each of the kinases. Based on this comparison it appears that the structure of the RSK2 NTKD ATP binding pocket is reasonable because we are able to closely superimpose the conformations of staurosporine and its derivative, Ro31-8820, bound to the different kinases (Fig. 1A). Therefore, we used this model to

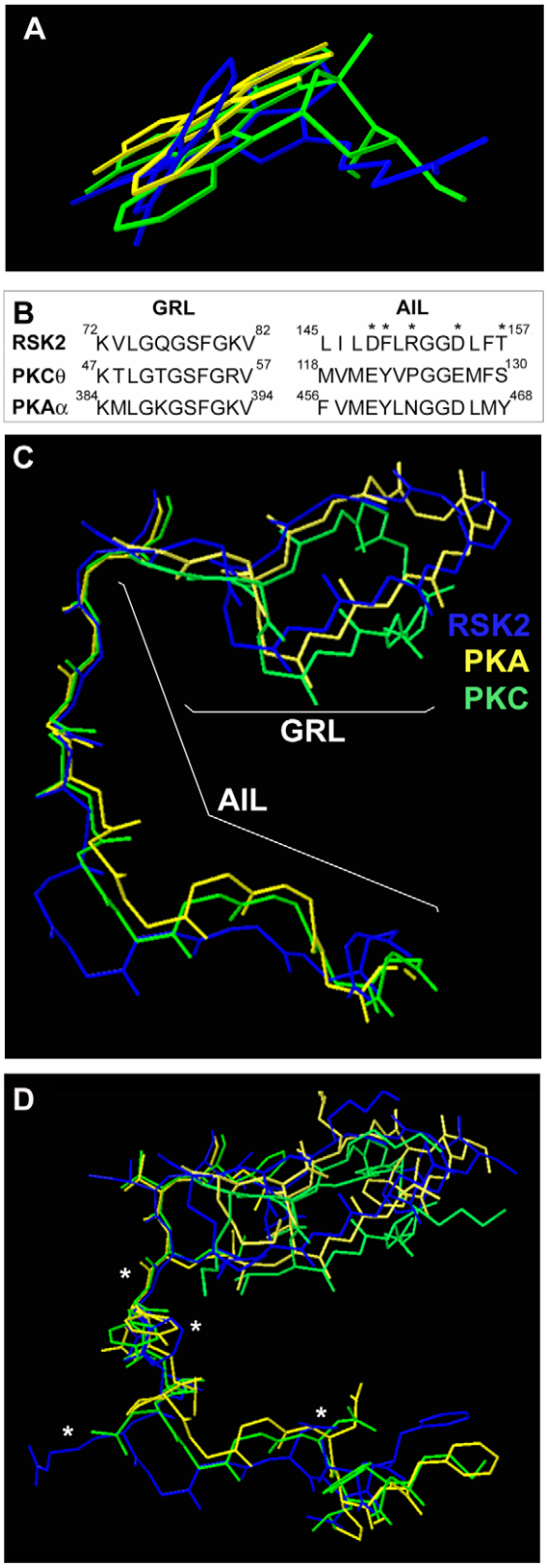

Figure 1. A model illustrating the unique features of the RSK2 NTKD ATP binding pocket. (A) The crystal structures of PKAα (1STC) and PKCθ (1XJD), both bound to staurosporine, were superimposed on the atomic model for RSK2 NTKD interacting with the staurosporine derivative, Ro31-8820. The superimposition of the compounds is shown. (B) The residues present in the adenosine-interacting loop (AIL) and the glycine-rich loop (GRL) for human RSK2 (U08316), PKAα (X07767), and PKCθ (X52479) are shown. The * indicates those residues whose alteration abrogates SL0101 binding. (C) As in A except the backbone of the polypeptide chains for PKA, PKC, and RSK2 comprising the AIL and the GRL are shown. (D) As in C except the side chains are also shown and the * indicates residues that were mutated.

study how the RSK NTKD interacts with SL0101. We demonstrated previously that a major determinant of specificity of RSK for SL0101 is provided by a unique sequence present in the ATP binding pocket in the NTKD of RSK.[2] This sequence is predicted to contact the adenosine moiety of ATP and is referred to as the adenosine-interacting loop (AIL). The AIL and the glycine-rich loop (GRL) are not contiguous in the primary sequence (Fig. 1B). The GRL interacts with the phosphates of ATP and is a major determinant in the affinity of interaction of kinases with ATP. The conformation of the AIL and the GRL present in the ATP binding pocket of RSK2 was compared with that of PKA and PKC by superimposing the structures. One view shows the backbone of the polypeptides (Fig. 1C) and the other view also shows the side chains (Fig. 1D). Based on our analysis the AIL in RSK2 would be farther away from the adenosine of ATP than in PKA and PKC. Thus, the ATP binding pocket of RSK2 has a different overall conformation than those of PKA and PKC. It is likely that both the differences in size of the ATP binding pocket as well as the residues that line the pocket are important in the specific interaction of the NTKD with SL0101 (**1**). To further understand the interaction of the NTKD with SL0101(**1**) we designed and synthesized various SL0101 derivatives and determined their affinity and specificity for inhibition of RSK activity.

2.2. Synthesis of SL0101 derivatives

The synthesis of the SL0101 analogues was generally carried out in a manner analogous to that reported for (**1**),[13] in which the requisite chalcone intermediate was oxidatively cyclized to afford the protected kaempferol moiety. Heterogeneous glycosylation conditions (Ag_2O) with the appropriate glycosyl bromide, followed by deprotection of the phenolic and carbohydrate hydroxyl groups, afforded the desired SL0101 analogues in a facile manner. The first analogue synthesized was triOH-SL0101 (**4**), which was obtained via deacetylation and debenzylation of fully protected SL0101 derivative **2**,[13] as shown in Scheme 1.

The synthesis of the ethylated analogue, Et-SL0101 (**6**), was carried out in a similar manner by ethylation (ethyl iodide, NaH) of the 3″ and 4″-OH groups of compound **3**, followed by hydrogenolysis of the benzyl ethers to afford the Et-SL0101 derivative (**6**) in 48% yield over two steps (Scheme 2).

The synthesis of 5-deoxy-SL0101 (**11**) was achieved utilizing the Algar–Flynn–Oyamada[14–16] reaction of the known chalcone **7** to afford 5-deoxykaempferol **8**[17] in one step (Scheme 3). Notably, this reaction only proceeds in good to moderate yield when the chalcone lacks functionality at C-5. Glycosylation with previously reported glycosyl bromide **9**[13] gave the fully protected 5-deoxy-SL0101 (**10**) in 62% yield. Debenzylation afforded 5-deoxy-SL0101 (**11**) in 96% yield.

The syntheses of 4′, 5, 7-trimethoxy-SL0101 (**16**), 4′, 7-dideoxy-SL0101 (**22**), and 7-deoxy-SL0101 (**27**) utilized the same methodology described for the previous analogues (vide supra); these are outlined in Scheme 4. Peracetylated-SL0101 (**28**) was obtained via peracetylation of tri-*O*-Ac-SL0101 (**29**)[18] in 95% yield (Scheme 5).

2.3. Acylation of the rhamnose moiety regulates affinity and specificity of SL0101 for RSK

To determine the importance of the rhamnose acetyl groups in the interaction with RSK we synthesized trihydroxy-SL0101 (**4**) and determined its IC_{50} for inhibition of RSK. The IC_{50} was identified by measuring the ability of various concentrations of trihydroxy-SL0101 (**4**) to inhibit RSK activity in an in vitro kinase assay

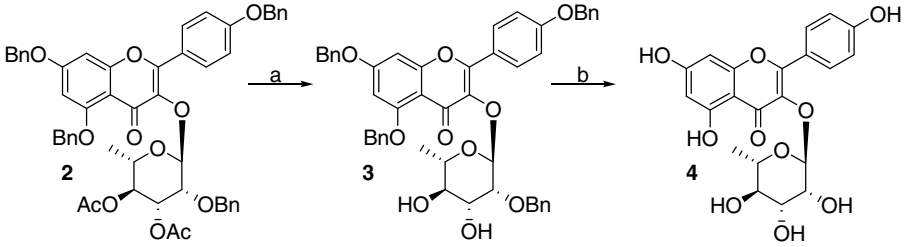

Scheme 1. Reagents: (a) K_2CO_3, 1:1 THF–MeOH (90%); (b) $Pd(OH)_2/C$, H_2, 1:1 THF–MeOH (80%).

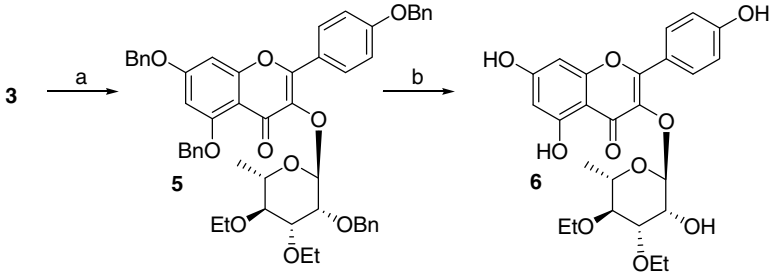

Scheme 2. Reagents and condition: (a) NaH, iodoethane, THF, reflux (48%); (b) $Pd(OH)_2/C$, H_2, 1:1 THF–MeOH (100%).

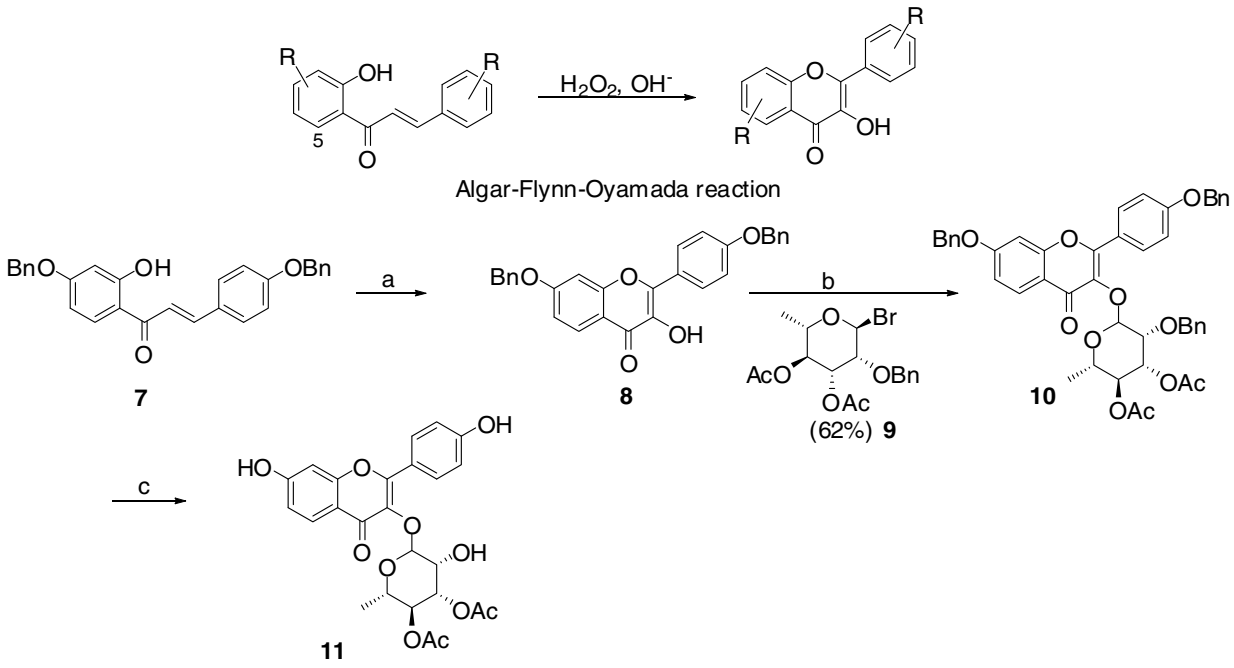

Scheme 3. Reagents and conditions: (a) H_2O_2, 5% aq. NaOH, EtOH, 1,4-dioxane (46%); (b) Ag_2O, **9**, 4 Å mol. sieves, CH_2Cl_2 (62%); (c) $Pd(OH)_2/C$, H_2, 1:1 THF–MeOH (96%).

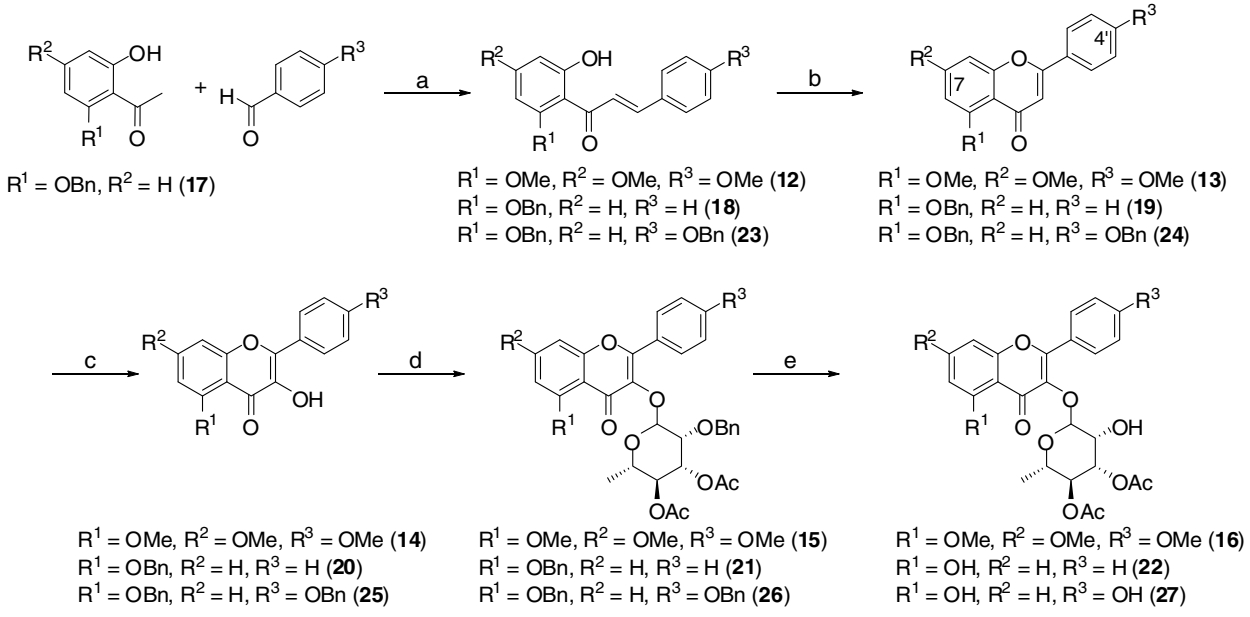

Scheme 4. Reagents and conditions: (a) 40% w/v KOH in MeOH, MeOH, reflux; (b) I_2, DMSO, 140 °C; (c) i—DMDO (0.05–0.1 M in acetone), CH_2Cl_2, 4 °C; ii—pTsOH, $CHCl_3$; (d) Ag_2O, **9**, 4Å mol. sieves, CH_2Cl_2; (e) $Pd(OH)_2/C$, H_2, 1:1 THF–MeOH.

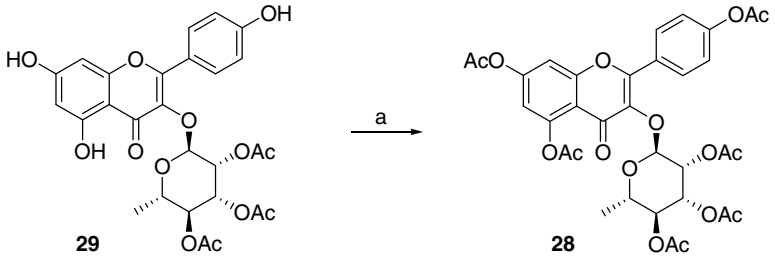

Scheme 5. Reagents and conditions: (a) Ac_2O, Et_3N, DMAP, CH_2Cl_2 (95%).

using recombinant, constitutively active RSK2.[2] The data were fit using nonlinear regression analysis; the IC_{50} value for trihydroxy-SL0101 (**4**) was >10-fold higher than that of SL0101 (**1**) (Fig. 2). To permit the direct comparison of the various derivatives with SL0101 we performed in vitro kinase assays using SL0101 (**1**) in parallel. The IC_{50} value for SL0101 (**1**) was in agreement with our previously published result.[18] Thus, these results clearly demonstrate that appropriate regioselective acetylation of the rhamnose moiety increases the affinity of RSK for SL0101 (**1**).

To investigate whether the nature of the *O*-substituent on the rhamnose moiety influenced the affinity of RSK for SL0101 (**1**) we synthesized Et-SL0101 (**6**) and found that its IC_{50} value for RSK inhibition was ~3-fold lower than that of SL0101 (**1**) (Fig. 2). Previously, we found that replacement of the acetyl groups on the rhamnose with butyryl groups, Bu-SL0101 (**30**), did not substantially alter the IC_{50}.[18] However, Bu-SL0101 (**30**) was not specific for inhibition of RSK.[18] To assess whether Et-SL0101 (**6**) was specific for inhibition of RSK activity we examined whether Et-SL0101 (**6**) preferentially inhibited the growth of MCF-7 compared to MCF-10A cells. We have reported previously that MCF-7 cells have become dependent on RSK activity for their growth, whereas inhibition of RSK activity in MCF-10A cells does not decrease their growth rate.[2] Therefore, this differential dependence on RSK activity for growth provides a convenient assay to assess the specificity of the various SL0101 derivatives for RSK. Previously, we found that at 100 μM Bu-SL0101 (**30**)

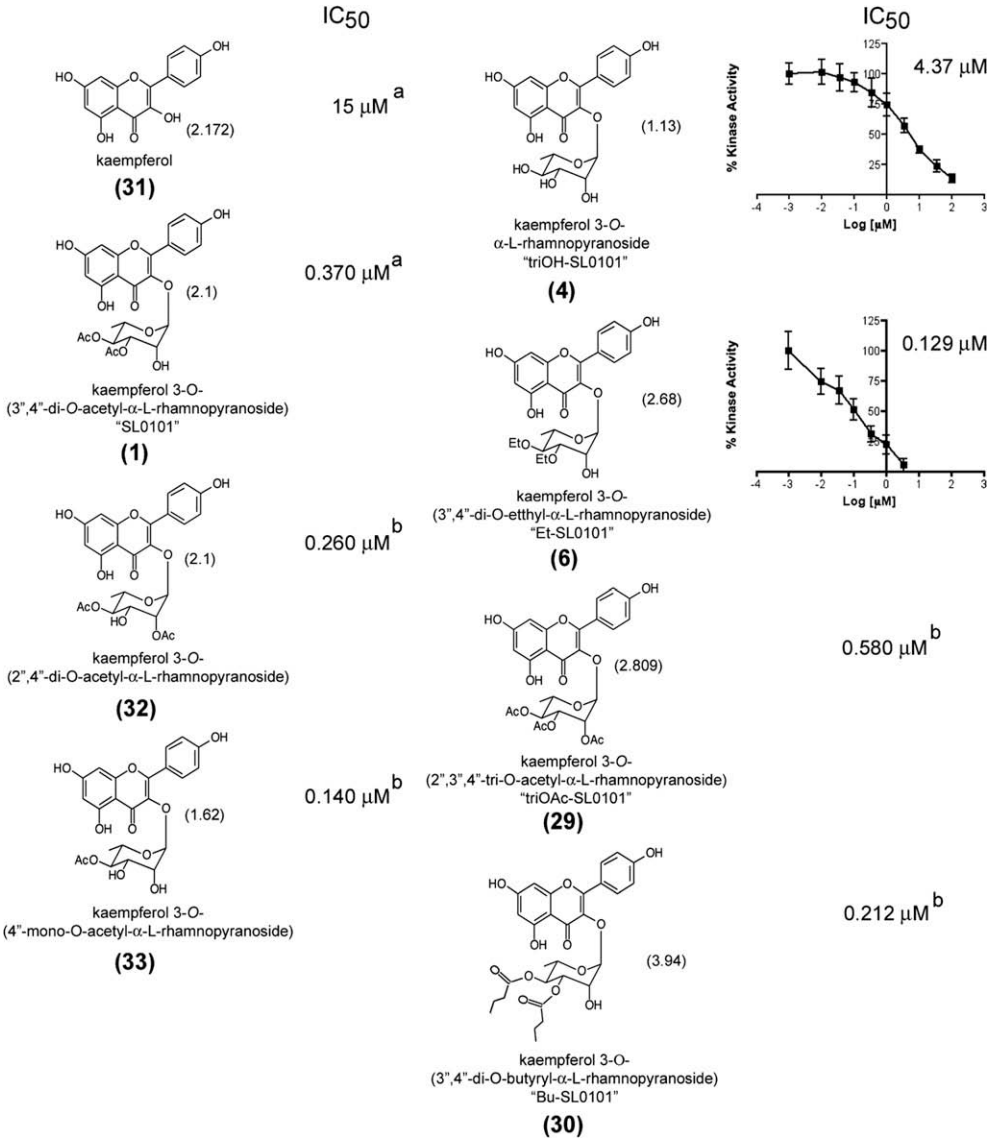

Figure 2. Alkylation of the rhamnose regulates the affinity of RSK for SL0101 in an in vitro kinase assay. The potencies of kaempferol, SL0101, and its derivatives in inhibiting RSK catalytic activity in vitro were measured. Kinase assays were performed using immobilized substrate. The reactions were initiated by the addition of 10 μM ATP (final concentration). Reactions were terminated after 30 min. All assays measured the initial reaction velocity. The extent of phosphorylation was determined using phosphospecific antibodies in combination with HRP-conjugated secondary antibodies. HRP activity was measured as described in the Experimental. Maximum and minimum activity is the relative luminescence detected in the presence of vehicle and 200 mM EDTA, respectively. *Points*, mean ($n = 2$ in quadruplicate); *bars* = SD. [a]IC_{50} values for compounds **1** and **31** were as reported.[2] [b]IC_{50} values for compounds **29**, **30**, **32**, and **33** were as reported.[18] The log *P* for each compound is indicated in unbolded parentheses.

inhibited both MCF-7 and MCF-10A cell proliferation.[18] Analysis of phosphoprotein profiles in the intact cell demonstrated that Bu-SL0101 (**30**), unlike SL0101 (**1**), inhibited the phosphorylation of a ~25 kDa protein, as detected by the anti-phospho AKT motif antibody.[18] These results demonstrated that Bu-SL0101 (**30**) is not specific for RSK, and also validated the differential growth assay as a measure of the specific inhibition of RSK activity. At all concentrations tested Et-SL0101 (**6**) was only slightly better at inhibiting the growth of MCF-7 compared to MCF-10A cells (Fig. 3). In contrast, triOH-SL0101 (**4**) was completely ineffective at inhibiting MCF-7 cell growth. To permit the direct comparison of the various derivatives with SL0101 we also performed proliferation assays in MCF-7 and MCF-10A cells using SL0101 (**1**). The results were similar to those reported previously in which concentrations of SL0101 (**1**) up to 200 μM did not affect MCF-10A cell growth, whereas MCF-7 cell growth was completely inhibited at doses >100 μM. Therefore, Et-SL0101 (**6**) is not specific for RSK even though its affinity for RSK is improved. Taken together, these results demonstrate that the acetyl groups on the rhamnose moiety regulate the specificity of SL0101 (**1**) for RSK.

2.4. The 4′, 5, and 7 hydroxyl groups on the kaempferol nucleus influence the affinity of RSK for SL0101

To determine the importance of the phenolic hydroxyl groups of the kaempferol moiety in RSK binding, we synthesized 5-deoxy-SL0101 (**11**), 4′, 7-dideoxy-SL0101 (**22**), and 7-deoxy-SL0101 (**27**). The IC_{50} value for 5-deoxy-SL0101 (**11**) was 24.6 μM; thus elimination of the 5-hydroxyl group resulted in a >65-fold reduction in affinity compared to SL0101 (**1**) (Fig. 4). These data demonstrate that the 5-hydroxyl group of SL0101 is essential for RSK binding with high affinity. Elimination

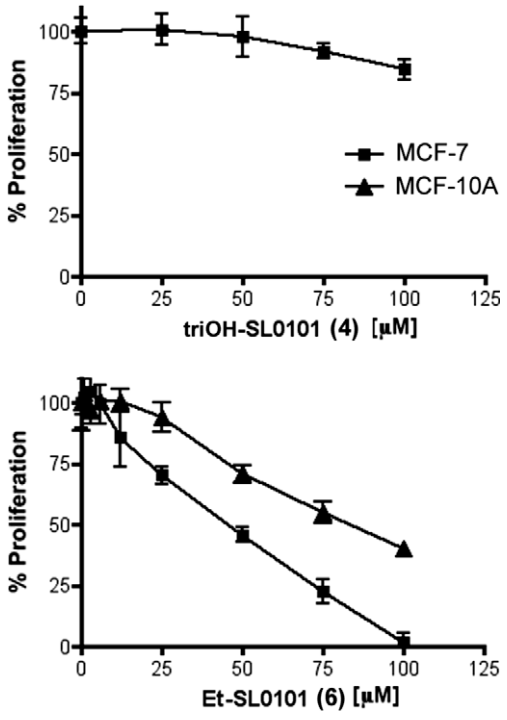

Figure 3. The nature of *O*-substitution of the rhamnose moiety regulates the specificity of SL0101 for inhibition of RSK activity in the intact cell. The potency of SL0101 derivatives as inhibitors of MCF-7 and MCF-10A cell proliferation was determined. The cell number was measured after 48 h of treatment. Values given are the fold proliferation as a percentage of that observed with vehicle-treated cells. *Points*, mean ($n = 2$ in quadruplicate); *bars* = SD.

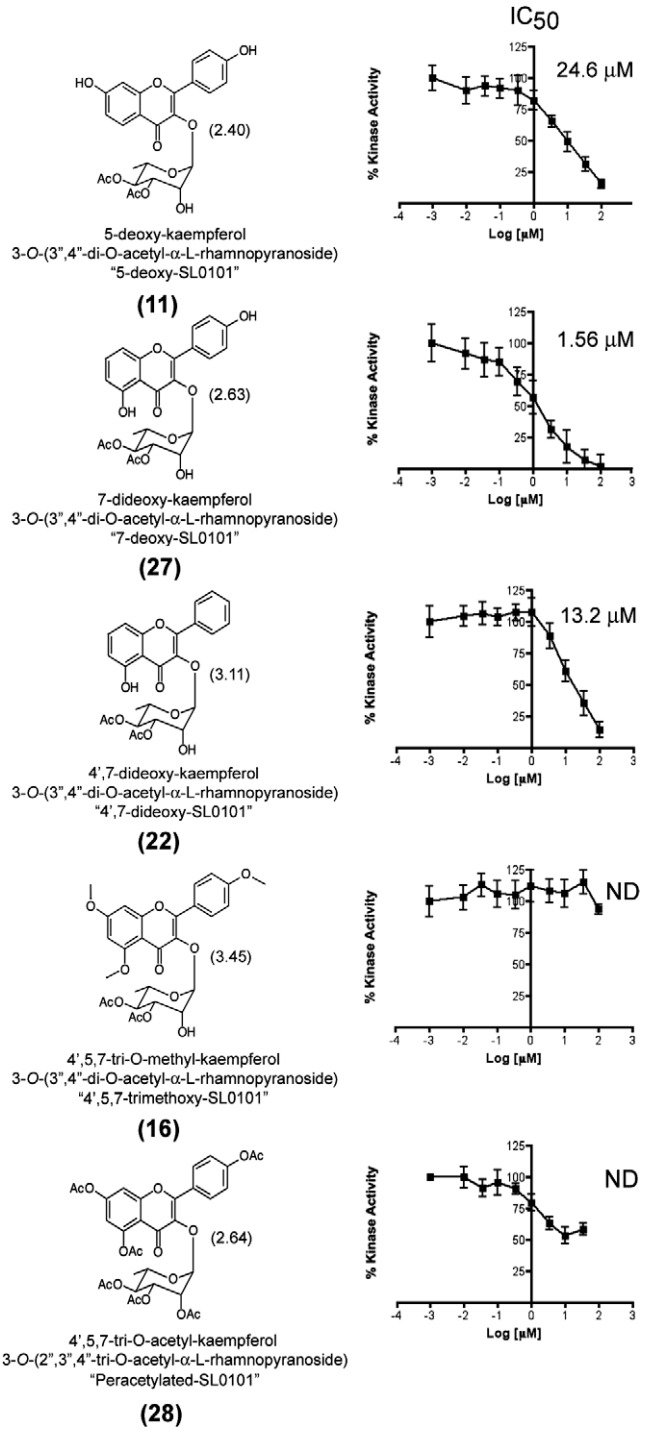

Figure 4. The hydroxyl groups on the kaempferol nucleus regulate the affinity of RSK for SL0101. The potency of the SL0101 derivatives as inhibitors of RSK catalytic activity in vitro was measured as described in Figure 2. The log *P* for each compound is indicated in unbolded parentheses. ND, not determined.

of the 7-hydroxyl group (**27**) increased the IC_{50} ~ 4-fold compared to that obtained with SL0101 (**1**) (Fig. 4). Removal of the 4′-hydroxyl group in addition to that of the 7-hydroxyl group (**22**) resulted in an IC_{50} of 13.2 μM (Fig. 4). The substantial decrease in affinity can be attributed mostly to the absence of the 4′-hydroxyl group (cf. **22** vs **27**). Thus, the 4′-, 5-, and 7-hydroxyl groups all contribute to the affinity of SL0101 for RSK.

It seems likely that loss of hydrogen bonding causes the decrease in affinity when the phenolic hydroxyl groups at the 4′, 5, and 7 positions of SL0101 are eliminated. To study this point further, the hydroxyl groups were *O*-methylated to disrupt any possible donor hydrogen bonding. 4′, 5, 7-Trimethoxy-SL0101 (**16**) was completely ineffective at inhibiting RSK activity (Fig. 4). It could be argued that the steric effect of the methoxyl group, rather than disruption of H-bonding, was responsible for the absence of RSK binding by 4′, 5, 7-trimethoxy-SL0101 (**16**). Another species studied was peracetylated SL0101 derivative **28**. From a steric perspective, the substituents on the 4′, 5, and 7-positions in **28** are larger than those in **16**, but the substantial dipole associated with the ester carbonyl moieties may provide an opportunity for new protein–ligand interactions not accessible with **16**, thus compensating for the putative loss of H-bonding interactions. It has already been shown that acetylation of the hydroxyl groups on the rhamnose moiety does not substantially alter the affinity of RSK for tri-*O*-Ac-SL0101 (**29**).[18] Thus, if RSK does not bind 4′, 5, 7-trimethoxy-SL0101 (**16**) purely due to steric constraints, it would be predicted that peracetylated-SL0101 (**28**) would also not bind to RSK. However, we found that RSK activity could be inhibited by ~50% using 10 μM peracetylated-SL0101 (**28**) (Fig. 4). It was not possible to perform a complete dose response curve with peracetylated-SL0101 (**28**) because of its limited solubility in aqueous solution. Nonetheless these results argue that residues in RSK hydrogen bond to the 5-hydroxyl group and the 4′- or 7-hydroxyl group, or both of these groups, in SL0101 (**1**).

To determine whether the 4′-, 5- or 7-hydroxyl groups also contributed to the specific inhibition of RSK by SL0101 we examined the ability of the derivatives to inhibit MCF-7 and MCF-10A cell growth. The 5-deoxy-SL0101 (**11**) was a poor inhibitor of MCF-7 proliferation causing only a 50% reduction at 100 μM (Fig. 5A), which was expected based on the low affinity of RSK for 5-deoxy-SL0101 (**11**). The specificity of 7-deoxy-SL0101 (**27**) and 4′, 7-dideoxy-SL0101 (**22**) for RSK at 100 μM was decreased in comparison to SL0101 (**1**) (Fig. 5A). However, at 75 μM both derivatives completely inhibited the growth of MCF-7 cells, whereas MCF-10A growth was decreased by only ~25–40%. Thus, both of these derivatives are more potent at 75 μM for inhibition of RSK activity in the proliferation assay than SL0101 (**1**). To directly assess the efficacy of these derivatives for inhibition of RSK activity in the intact cell, their ability to decrease the mitogen-induced phosphorylation of the RSK substrate, p140, was analyzed. In these assays MCF-7 cells were pre-treated for 2 h with the indicated concentration of inhibitor and then stimulated with the mitogen, phorbol myristate acetate (PMA), for 20 min.[2] In agreement with our previous results the phosphorylation of p140 is stimulated by PMA and inhibited by SL0101 (**1**) and U0126, an inhibitor of mitogen activated kinase kinase, an upstream activator of RSK (Fig. 5B). A 2-h pretreatment with 75 μM 7-deoxy-SL0101 (**27**) abolished the mitogen-induced phosphorylation of p140, whereas 4′, 7-dideoxy-SL0101 (**22**) inhibited it by ~50%. It is likely that 7-deoxy-SL0101 (**27**) is more effective at inhibiting p140 phosphorylation than 4′, 7-dideoxy-SL0101 (**22**) due to its higher affinity. At 75 μM both 4′,7-dideoxy-SL0101 (**22**) and 7-deoxy-SL0101 (**27**) specifically inhibit RSK activity, which argues that the 4′ and 7 hydroxyl groups do not substantially contribute to the specificity of SL0101 (**1**) for RSK.

3. Discussion

We have shown that the ability of RSK to interact with SL0101 depends on the sugar moiety because RSK has a 40-fold greater affinity for SL0101 (**1**) compared to kaempferol (**31**) (Fig. 2).[2] During the isolation of SL0101 we also identified compounds that differ from SL0101 (**1**) only in the number and position of the acetyl groups on the rhamnose moiety ((**32**) and (**33**)) and we found that RSK was able to bind these compounds with similar in vitro affinities as SL0101 (**1**) (Fig. 2).[18] Furthermore, acylation of all the hydroxy groups on the rhamnose to generate tri-*O*-Ac-SL0101 (**29**) did not substantially alter the inhibitory potency or specificity for inhibiting RSK activity in vitro (Fig. 2).[18] However, trihydroxy-SL0101 (**4**) was found to be much less potent at inhibiting RSK than SL0101 (**1**), indicating that some of the sugar acyl groups must be required for enzyme binding.

Our studies further suggest that the efficacy of SL0101 in intact cells could be improved by increasing its hydrophobic character. This conclusion is based on our observations that 7-deoxy-SL0101 (**27**) and 4′, 7-dideoxy-SL0101 (**22**) are more potent RSK inhibitors than SL0101 in the intact cell despite their lower in vitro affinity for RSK. It is highly likely that 7-deoxy-SL0101 (**27**) and 4′, 7-dideoxy-SL0101 (**22**) are more potent than SL0101 (**1**) in the proliferation assay, which occurs over a longer time period, because their increased hydrophobic character facilitates cellular uptake, which compensates for their lower affinity. Additionally, it was observed that 15 μM peracetylated SL0101 (**28**) inhibited MCF-7 cell proliferation by ~50% while having no effect on MCF-10A cell proliferation (data not shown). We attempted to use Cremophor to aid in solubilizing the peracetylated-SL0101 (**28**) in the proliferation assays but nonspecific toxicity was observed with percentages of Cremophor >1%, which were needed to keep the peracetylated-SL0101 (**28**) soluble at concentrations >15 μM. Thus even though peracetylated-SL0101 (**28**) is less effective than SL0101 (**1**) in the in vitro kinase assay, its greater hydrophobic character makes it more potent in the intact cell. Taken together, these results suggest that the efficacy of SL0101 (**1**) is limited in the intact cell by cellular uptake. It is of inter-

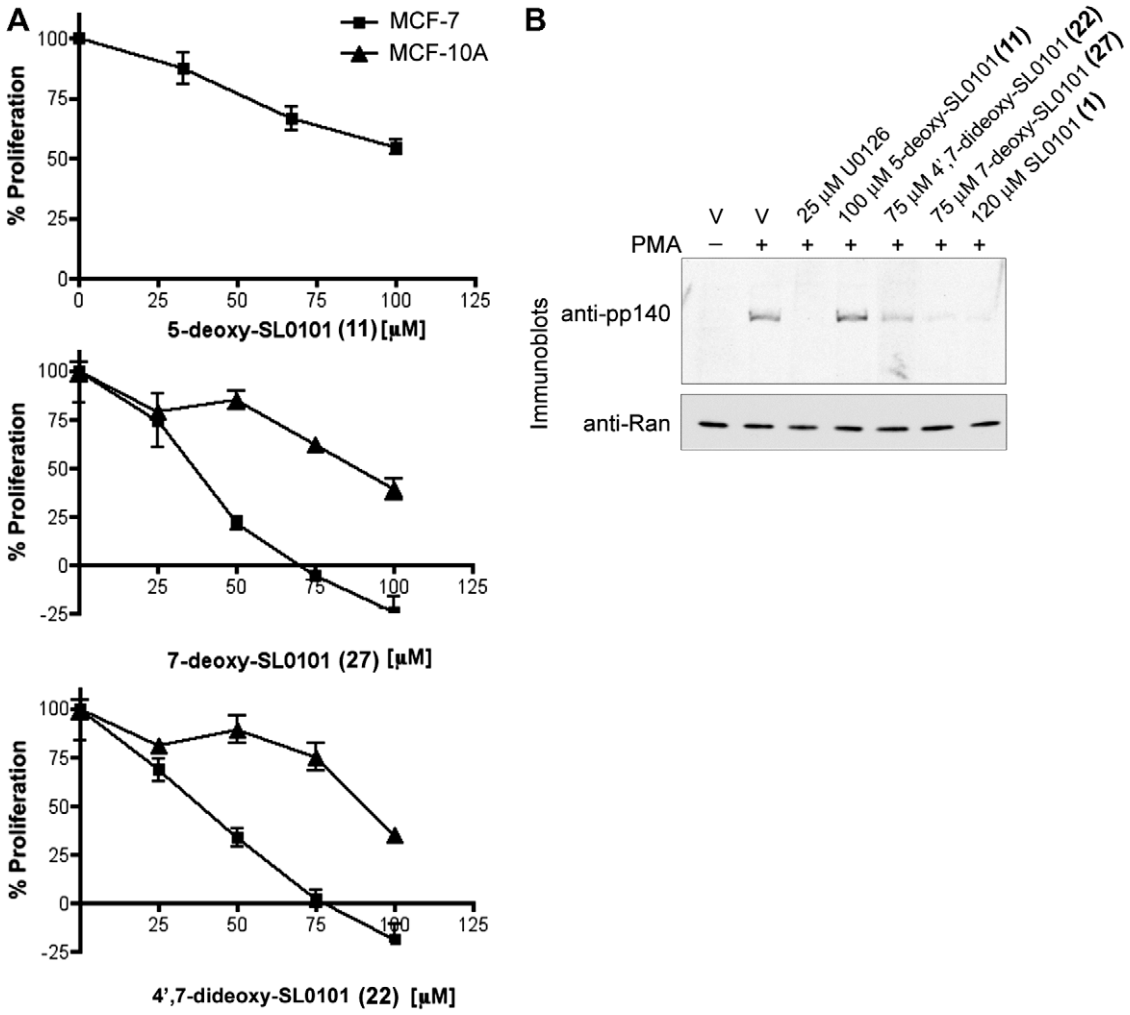

Figure 5. Increasing hydrophobic character of SL0101 improves potency in the intact cell. (A) The efficacy of the SL0101 derivatives as inhibitors of MCF-7 and MCF-10A cell proliferation was determined as in Figure 3. (B) The potency of the SL0101 derivatives as inhibitors of RSK activity in intact cells was analyzed. Serum-deprived MCF-7 cells were pre-incubated with vehicle, or the indicated concentration of inhibitor for 2 h. Cells were treated with 500 nM PMA or vehicle for 20 min prior to lysis. Protein concentration of lysates was measured and lysates were electrophoresed, transferred, and immunoblotted. Equal loading of lysate is demonstrated by the anti-Ran immunoblot.

est to note that the acetyl groups present in SL0101 (**1**) and peracetylated-SL0101 (**28**) may well be hydrolyzed by ubiquitous intracellular esterases. Thus, both compounds could potentially be metabolized to triOH-SL0101 (**4**), which is a less effective inhibitor of RSK activity than SL0101 (**1**) and is ineffective at inhibiting MCF-7 cell growth. Therefore, the efficacy of SL0101 (**1**) in the intact cell is most likely limited both by cellular uptake and metabolism.

The hydroxyl groups, in particular the 5-OH and 4′-OH groups on the kaempferol nucleus, are important determinants of the affinity of SL0101 for RSK. It is likely that these groups are involved in hydrogen bonding because methylating the hydroxy groups eliminated inhibition of RSK activity. Interestingly, the 4′- and 7-OH groups do not appear to contribute critically to the specific interaction of RSK with SL0101 because both 7-deoxy-SL0101 (**27**) and 4′,7-dideoxy-SL0101 (**22**) were able to specifically inhibit RSK activity in the proliferation assay at 75 μM concentration.

In the RSK2 NTKD atomic model described by Nguyen et al.[10] SL0101 (**1**) is positioned so that the kaempferol nucleus is located near the AIL and the rhamnose moiety is near the GRL. Based on our structural analysis, it is likely that residues within the AIL are involved in hydrogen bonding with the hydroxyl groups on the kaempferol nucleus of SL0101 (**1**). Furthermore, it appears that alkylation of the rhamnose moiety can facilitate the interaction with the GRL of a number of different kinases. However, the acetylation of the rhamnose moiety confers specificity for RSK.

These studies should aid in the design of SL0101 (**1**) derivatives having optimized pharmacokinetic and pharmacodynamic properties. A dihydropteridinone derivative, BI-D1870, has recently been identified that also inhibits RSK activity.[19] SL0101 and BI-D1870 are ATP competitors that directly inhibit the phosphorylation of exogenous substrates through inhibition of RSK NTKD activity. Pyrrolo[2,3-d]pyrimidine derivatives that are irreversible inhibitors of the RSK CTKD

have also been reported.[20] These inhibitors are thought to inhibit RSK NTKD activity indirectly by preventing its activation by the CTKD. The in vivo potencies of BI-D1870 and the pyrrolo[2,3-d]pyrimidine derivatives as inhibitors of RSK activity have not yet been reported.

In addition to its involvement in various cancers, inappropriate RSK activity has been implicated in the etiology of a number of other diseases including cardiomyopathy, infection, and lead poisoning.[21–23] Further, elevated activity of MAPK, the immediate upstream RSK activator, has also been shown in various neural and heart pathologies, inflammation, and Borna disease.[24–35] It is possible that RSK is also involved in these disorders through activation of its kinase activity by MAPK. Therefore, it is possible to envision a number of potential clinical uses for RSK inhibitors. However, RSK2 is important in normal development and has been associated with Coffin-Lowry syndrome.[36] In this syndrome patients have an X-linked mental retardation condition and skeletal abnormalities. Some of the pathology associated with this syndrome may be due to the fact that the patients express truncated mutants of RSK2. These mutants may have functions that differ from wild-type RSK2. In a RSK2 mouse knockout model MAPK activity is elevated and it is thought that RSK2 may act as a negative regulator of MAPK activity.[37] Increased MAPK activity would have wide ranging biological effects and therefore might be deleterious.[1] However, it is not clear whether this feedback loop exists only as a consequence of the loss of the RSK2 protein during development. Interestingly, in Drosophila, flies that have a kinase-dead RSK mutant instead of wild-type RSK develop normally.[38] In comparison, flies that are null for RSK have increased MAPK activity and are defective. These results suggest that it may be possible to inhibit RSK activity without deleterious consequences to a developing organism. Furthermore, our data suggest that RSK activity is not required for the maintenance of normal homeostasis in nontumorigenic cells.[2] Thus, it is possible that an inhibitor of RSK activity may be well tolerated in vivo.

4. Experimental

4.1. Modeling

The models were of generated by Swiss PdbViewer 3.70b0 and are based on the coordinates under Protein Data Bank entry codes 1STC for PKAα[11] and 1XJD for PKCθ,[12] both bound to staurosporine. The models for PKAα and PKCθ were superimposed on the atomic model for RSK2 interacting with the staurosporine derivative, Ro31-8820.[10]

4.2. Chemistry

Reagents and solvents were reagent grade and were used without further purification. Methylene chloride was distilled from calcium hydride. Anhydrous grade THF was purchased from VWR. All reactions involving air- or moisture- sensitive reagents or intermediates were performed under a nitrogen or argon atmosphere. Flash chromatography was performed using Silicycle 40–60 mesh silica gel. Analytical TLC was performed using 0.25 mm EM silica gel 60 F_{250} plates that were visualized by irradiation (254 nm) or by staining with Hanessian's stain (cerium molybdate). Optical rotations were obtained using a Jasco digital polarimeter. ^{1}H and ^{13}C NMR spectra were obtained using 300 and 500 MHz Varian instruments. Chemical shifts are reported in parts per million (ppm, δ) referenced to the residual ^{1}H resonance of the solvent ($CDCl_3$, 7.26 ppm; DMSO-d_6, 2.49 ppm). ^{13}C spectra were referenced to the residual ^{13}C resonance of the solvent ($CDCl_3$, 77.3 ppm; DMSO-d_6, 39.5 ppm). Splitting patterns are designated as follows: s, singlet; br, broad; d, doublet; dd, doublet of doublets; t, triplet; q, quartet; m, multiplet. High resolution mass spectra were obtained at the Michigan State University-NIH Mass Spectrometry Facility. Log P values were calculated using Molinspiration Property Calculation Service (www.molinspiration.com).

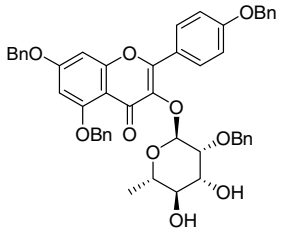

4.2.1. 4′,5,7-Tri-*O*-benzyl-kaempferol 3-*O*-(2″-*O*-benzyl-α-L-rhamnopyranoside) (3). To a solution containing 0.08 g (0.09 mmol) of **2** in 5 mL of 1:1 THF–MeOH was added catalytic K_2CO_3 and the reaction mixture was stirred at room temperature under a N_2 atmosphere for 3 h. The reaction mixture was then filtered though a Celite® pad and washed with ethyl acetate, and the filtrate was concentrated under diminished pressure. The residue was purified by flash chromatography on a silica gel column (25 × 3 cm). Elution with 1:1 hexanes–ethyl acetate gave **3** as a colorless foam: yield 0.061 g (90%); silica gel TLC R_f 0.19 (1:1 hexanes–ethyl acetate); $[\alpha]_D^{20}$ −40.1 (*c* 1.0, $CHCl_3$); ^{1}H NMR ($CDCl_3$) δ 0.95 (d, 3H, *J* = 6.0 Hz), 2.33 (br s, 2H), 3.25 (m, 1H), 3.36 (t, 1H, *J* = 9.3 Hz), 3.74 (m, 1H), 4.38 (d, 1H, *J* = 1.5 Hz), 4.71 (d, 1H, *J* = 11.7 Hz), 4.88 (d, 1H, *J* = 11.7 Hz), 5.09 (s, 2H), 5.14 (s, 2H), 5.26 (s, 2H), 5.78 (s, 1H), 6.49 (s, 1H), 6.58 (s, 1H), 7.10 (d, 1H, *J* = 7.5 Hz), 7.30–7.43 (m, 19H), 7.62 (d, 2H, *J* = 7.5 Hz) and 7.81 (d, 2H, *J* = 8.4 Hz); ^{13}C NMR ($CDCl_3$) δ 17.36, 70.00, 70.32, 70.73, 70.99, 71.43, 72.73, 73.54, 77.50, 77.85, 94.16, 98.44, 98.76, 110.25, 114.93, 123.44, 126.83, 127.68, 127.86, 128.21, 128.37, 128.48, 128.70, 128.80, 128.91, 129.01, 130.71, 135.84, 136.60, 138.07, 138.30, 154.56, 159.12, 159.99, 160.67, 163.10 and 173.63; mass spectrum (FAB), *m/z* 793.3010 $(M+H)^+$ ($C_{49}H_{45}O_{10}$ requires 793.3013).

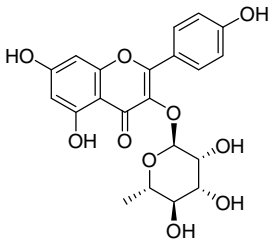

4.2.2. Kaempferol 3-*O*-α-L-rhamnopyranoside (trihydroxy-SL0101) (4). A suspension containing 0.06 g (0.07 mmol) of **3** and 0.010 g of $Pd(OH)_2/C$ in 5 mL of 1:1 THF–MeOH was purged three times with H_2. The reaction vessel was kept under a H_2 atmosphere for 1 h, then filtered through a Celite® pad and washed with ethyl acetate. The filtrate was concentrated under diminished pressure to afford a solid. Product **4** was pure and further purification was not necessary: yield 0.024 g (80%); silica gel TLC R_f 0.15 (1:1:0.1 hexanes–ethyl acetate–methanol); $[\alpha]_D^{20}$ −111.4 (*c* 0.8, $CHCl_3$); ^1H NMR (CD_3OD) δ 0.89 (d, 3H, *J* = 5.4 Hz), 2.43 (m, 1H), 2.46 (t, 1H, *J* = 7.8 Hz), 3.69 (m, 1H), 4.19 (m, 1H), 4.32 (t, 1H, *J* = 6.9 Hz), 5.34 (d, 1H, *J* = 1.5 Hz), 6.16 (d, 1H, *J* = 1.8 Hz), 6.33 (d, 1H, *J* = 1.8 Hz), 6.91 (d, 2H, *J* = 8.7 Hz) and 7.72 (d, 2H, *J* = 8.7 Hz); ^{13}C NMR (CD_3OD) δ 17.62, 71.94, 72.01, 72.16, 73.28, 95.22, 100.40, 103.47, 104.88, 116.03, 122.98, 132.34, 135.06, 158.91, 159.47, 161.50, 163.07, 166.42 and 178.56; mass spectrum (FAB), *m/z* 433.1136 $(M+H)^+$ ($C_{21}H_{21}O_{10}$ requires 433.1134).

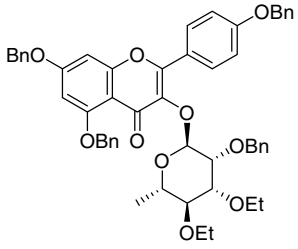

4.2.3. 4′,5,7-Tri-*O*-benzyl-kaempferol 3-*O*-(2″-*O*-benzyl-3″,4″-di-*O*-ethyl-α-L-rhamnopyranoside) (5). To a solution containing 0.10 g (0.13 mmol) of **3** in 5 mL of anhydrous THF at 0 °C was added 0.02 g (0.51 mmol) of a 60% dispersion of NaH in mineral oil. The reaction mixture was stirred at this temperature for 15 min, then 0.12 g (0.06 mL, 0.76 mmol) of iodoethane was added and the reaction mixture was heated to reflux for 20 h. The cooled reaction mixture was quenched with saturated aq NH_4Cl and diluted with ether. The aqueous layer was extracted with three 10-mL portions of ether. The combined organic layer was washed with two 15-mL portions of brine, dried ($MgSO_4$), and concentrated under diminished pressure. The resulting residue was purified by flash chromatography on a silica gel column (25 × 3 cm). Elution with 6:1 hexanes–ethyl acetate gave **5** as a colorless oil: yield 0.053 g (48%); silica gel TLC R_f 0.46 (2:1 hexanes–ethyl acetate); ^1H NMR ($CDCl_3$) δ 0.94 (d, 3H, *J* = 5.4 Hz), 1.17 (m, 6H), 3.26 (m, 2H), 3.46 (q, 2H, *J* = 6.9 Hz); 3.60 (m, 2H), 3.83 (m, 1H), 4.41 (m, 1H), 4.81 (m, 2H), 5.08 (s, 2H), 5.14 (s, 2H), 5.25 (s, 2H), 5.52 (s, 1H), 6.49 (d, 1H, *J* = 1.8 Hz), 6.55 (d, 1H, *J* = 2.1 Hz), 7.07 (d, 2H, *J* = 9.0 Hz), 7.23–7.47 (m, 16H), 7.50 (d, 2 H, *J* = 7.2 Hz), 7.64 (d, 2H, *J* = 7.5 Hz) and 7.80 (d, 2H, *J* = 8.7 Hz); ^{13}C NMR ($CDCl_3$) δ 15.88, 16.08, 17.73, 65.33, 68.31, 70.17, 70.37, 70.72, 71.00, 72.53, 75.23, 79.25, 79.64, 94.12, 98.38, 100.33, 110.29, 114.90, 123.62, 126.87, 127.58, 127.65, 127.87, 128.14, 128.35, 128.47, 128.69, 128.80, 128.93, 129.01, 130.74, 135.87, 136.65, 136.70, 138.82, 138.93, 154.54, 159.11, 160.01, 160.59, 163.04 and 173.68.

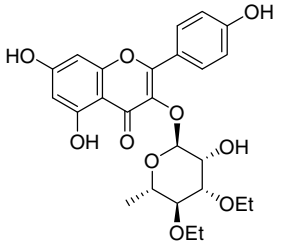

4.2.4. Kaempferol 3-*O*-(3″,4″-di-*O*-ethyl-α-L-rhamnopyranoside) (Et-SL0101) (6). A suspension containing 0.04 g (0.05 mmol) of **5** and 0.02 g of $Pd(OH)_2/C$ in 6 mL of 1:1 THF–MeOH was purged three times with H_2. The reaction vessel was kept under a H_2 atmosphere for 1 h, then filtered through a Celite® pad and washed with ethyl acetate. The filtrate was concentrated under diminished pressure. The residue was purified by flash chromatography on a silica gel column (20 × 2 cm). Elution with 1:1:0.1 hexanes–ethyl acetate–methanol gave **6** as a colorless oil: yield 0.02 g (100%); silica gel TLC R_f 0.39 (1:1:0.1 hexanes–ethyl acetate–methanol); $[\alpha]_D^{20}$ −115.8 (*c* 1.1, ethyl acetate); ^1H NMR (acetone-d_6) δ 0.99 (d, 3H, *J* = 6.3 Hz), 1.16 (t, 3H, *J* = 6.9 Hz), 1.28 (t, 3H, *J* = 6.9 Hz), 3.23 (t, 1H, *J* = 9.3 Hz), 3.47 (m, 1H), 3.63 (m, 3H), 3.82 (m, 2H), 4.04 (br s, 1H), 4.40 (m, 1H), 5.58 (d, 1H, *J* = 1.8 Hz), 6.35 (d, 1H, *J* = 1.8 Hz), 6.56 (d, 1H, *J* = 2.1 Hz), 7.10 (d, 2H, *J* = 8.7 Hz), 7.94 (d, 2H, *J* = 8.7 Hz), 9.47 (br s, 2H) and 12.80 (s, 1H); ^{13}C NMR (acetone-d_6) δ 15.95, 16.08, 17.93, 65.47, 68.08, 68.93, 70.45, 79.81, 80.12, 94.54, 99.53, 102.53, 105.81, 116.26, 122.52, 131.71, 135.69, 157.97, 158.37, 160.87, 163.20, 164.89 and 179.26; mass spectrum (FAB), *m/z* 489.1762 $(M+H)^+$ ($C_{25}H_{29}O_{10}$ requires 489.1760).

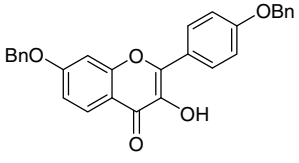

4.2.5. 4′,7-Di-*O*-benzyl-5-deoxykaempferol (8).[17] To a stirred suspension containing 2.00 g (4.58 mmol) of 1-(4-benzoxy-2-hydroxyphenyl)-3-(4-benzoxyphenyl) propenone (**7**) in 60 mL of EtOH was added 18 mL of dioxane, followed by 2 mL of H_2O_2 and 16 mL of 5% aqueous NaOH. The reaction mixture was stirred at room temperature overnight, then heated to 50 °C for 3 h. The cooled reaction mixture was poured into 200 mL of H_2O and acidified with 1 N HCl. The yellow precipitate was collected by filtration and washed with hot EtOH. The insoluble solid was collected and dried to afford **8** as a light yellow solid: yield 0.85 g (46%); mp 208–210 °C, lit.[17] mp 210–212 °C; silica gel TLC R_f 0.65 (1:1 hexanes–ethyl acetate); ^{1}H NMR (DMSO-d_6) δ 5.22 (s, 2H), 5.28 (s, 2H), 7.12 (dd, 1H, J = 8.7 and 1.8 Hz), 7.22 (d, 2H, J = 9.0 Hz), 7.36–7.50 (m, 11H), 8.01 (d, 1H, J = 8.7 Hz), 8.18 (d, 2H, J = 8.7 Hz) and 9.37 (br s, 1H).

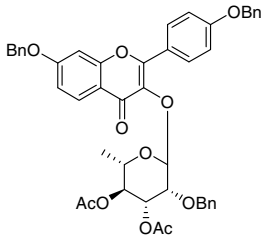

4.2.6. 4′,7-Di-*O*-benzyl-5-deoxykaempferol 3-*O*-(2″-*O*-benzyl-3″,4″-di-*O*-acetyl-α-L-rhamnopyranoside) (10). To a stirred suspension containing 0.10 g (0.24 mmol) of **8**, 0.11 g (0.48 mmol) of Ag_2O, and 4Å molecular sieves in 5 mL of CH_2Cl_2 was added 0.12 g (0.31 mmol) of 3,4-di-*O*-acetyl-2-*O*-benzyl-α-L-rhamnopyranosyl bromide (**9**)[13] as a solution in 5 mL of CH_2Cl_2. The reaction mixture was allowed to stir at room temperature for 4 h, then diluted with 20 mL of CH_2Cl_2 and filtered through a Celite® pad. The filtrate was concentrated under diminished pressure and the residue was purified by flash chromatography on a silica gel column (25 × 3 cm). Elution with 3:1 hexanes–ethyl acetate gave **10** as a colorless solid: yield 0.11 g (62%); silica gel TLC R_f 0.39 (2:1 hexanes–ethyl acetate); $[\alpha]_D^{22}$ −81.3 (*c* 0.1, $CHCl_3$); ^{1}H NMR ($CDCl_3$) δ 0.87 (d, 3H, J = 6.3 Hz), 1.96 (s, 3H), 1.98 (s, 3H), 3.44 (m, 1H), 4.31 (d, 1H, J = 1.5 Hz), 4.57 (d, 1H, J = 12.3 Hz), 4.78 (d, 1H, J = 12.3 Hz), 5.14 (m, 6H), 5.28 (dd, 1H, J = 10.2 and 3.3 Hz), 5.73 (s, 1H), 6.97 (br s, 1H), 7.05 (d, 1H, J = 8.7 Hz), 7.12 (d, 2H, J = 8.4 Hz), 7.40 (m, 14H), 7.87 (d, 2H, J = 8.4 Hz) and 8.13 (d, 1H, J = 9.0 Hz); ^{13}C NMR ($CDCl_3$) δ 17.42, 21.04, 21.11, 68.50, 70.35, 70.78, 71.26, 72.90, 75.78, 77.78, 98.80, 101.32, 115.05, 115.24, 118.43, 123.52, 127.42, 127.53, 127.72, 127.92, 128.21, 128.28, 128.45, 128.64, 128.93, 129.00, 130.84, 135.91, 136.53, 137.34, 138.09, 156.75, 157.21, 160.85, 163.33, 170.03, 170.40 and 173.99; mass spectrum (FAB), *m*/*z* 771.2803 $(M+H)^+$ ($C_{46}H_{43}O_{11}$ requires 771.2806).

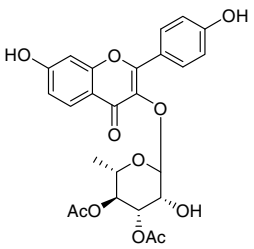

4.2.7. 5-Deoxykaempferol 3-*O*-(3″,4″-di-*O*-acetyl-α-L-rhamnopyranoside) (5-deoxy-SL0101) (11). A suspension containing 0.10 g (0.14 mmol) of **10** and 0.08 g of $Pd(OH)_2$/C in 5 mL of 1:1 THF–MeOH was purged with H_2 and kept under a H_2 atmosphere for 1 h. The reaction mixture was then diluted with ethyl acetate and filtered through a Celite® pad. The filtrate was concentrated under diminished pressure to give **11** as a light brown solid: yield 0.065 g (96%); silica gel TLC R_f 0.24 (1:1:0.1 hexanes–ethyl acetate–methanol); $[\alpha]_D^{23}$ −130.2 (*c* 0.6, MeOH); ^{1}H NMR (DMSO-d_6) δ 0.67 (d, 3H, J = 12.9 Hz), 1.95 (s, 3H), 1.99 (s, 3H), 3.27 (m, 1H), 4.22 (br s, 1H), 4.94 (m, 1H), 4.98 (dd, 1H, J = 10.2 and 2.7 Hz), 5.38 (d, 1H, J = 1.5 Hz), 5.65 (br s, 1H), 6.89 (d, 2H, J = 3.3 Hz), 6.91 (d, 2H, J = 8.7 Hz), 7.71 (d, 2H, J = 8.4 Hz), 7.90 (d, 1H, J = 8.7 Hz) and 10.50 (br s, 2H); ^{13}C NMR (DMSO-d_6) δ 17.03, 20.54, 20.78, 67.37, 67.76, 69.77, 71.05, 100.45, 102.19, 115.12, 115.40, 116.19, 120.85, 126.85, 126.74, 130.44, 135.41, 156.36, 156.62, 159.89, 162.76, 169.64, 170.01, 170.36 and 172.75; mass spectrum (FAB), *m*/*z* 501.1395 $(M+H)^+$ ($C_{25}H_{25}O_{11}$ requires 501.1397).

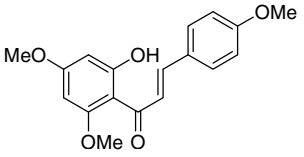

4.2.8. *E*-3-(4-Methoxyphenyl)-1-(2,4-bismethoxy-6-hydroxyphenyl)propenone (12).[39] To a solution containing 3.0 g (1.03 mmol) of 4′,5,7-trihydroxyflavanone in 50 mL of acetone was added 4.31 g (34.2 mmol) of dimethyl sulfate followed by 6.18 g (44.1 mmol) of K_2CO_3. The reaction mixture was heated to reflux under N_2 overnight then the solvent was concentrated under diminished pressure and the residue was redissolved in ethyl acetate. The organic layer was then washed with two 100-mL portions of brine, one 100-mL portion of 1 N HCl, dried ($MgSO_4$), and concentrated under diminished pressure. Purification by flash chromatography on a silica gel column (25 × 4 cm) and elution with 2:1 hexanes–ethyl acetate gave **12** as a yellow solid: yield 1.72 g (50%); mp 113–114 °C, lit.[39] mp 113–114 °C; silica gel TLC R_f 0.45 (2:1 hexanes–ethyl acetate); ^{1}H NMR ($CDCl_3$) δ 3.80 (s, 3H), 3.82 (s, 3H), 3.88 (s, 3H), 5.92 (d, 1H, J = 2.4 Hz), 6.07 (d, 1H, J = 2.4 Hz),

6.90 (d, 2H, J = 9.0 Hz), 7.54 (d, 2H, J = 9.0 Hz), 7.77 (s, 2H) and 14.45 (s, 1H); ^{13}C NMR ($CDCl_3$) δ 55.60, 55.76, 56.02, 91.37, 93.99, 114.55, 125.27, 128.46, 130.32, 142.66, 161.56, 162.65, 166.23, 168.59 and 192.75.

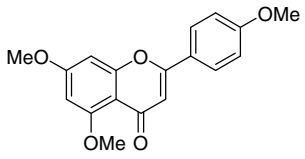

4.2.9. 5,7-Dimethoxy-2-(4-(methoxy)phenyl)-4*H*-chromen-4-one (13).[40] To a solution containing 1.40 g (4.53 mmol) of **12** in 50 mL of DMSO was added 0.12 g (0.45 mmol) of I_2. The reaction mixture was heated to reflux overnight under N_2, then cooled to room temperature, diluted with 200 mL ethyl acetate, and washed with two 100-mL portions of 1 N HCl. The organic layer was separated, dried ($MgSO_4$), and concentrated under diminished pressure. The residue was purified by flash chromatography on a silica gel column (28 × 4 cm). Elution with 1:2 hexanes–ethyl acetate gave **13** as an off-white solid: yield 1.21 g (86%); mp 153–155 °C, lit.[40] mp 158–159 °C; silica gel TLC R_f 0.10 (1:2 hexanes–ethyl acetate); ^{1}H NMR ($CDCl_3$) δ 3.83 (s, 3H), 3.86 (s, 3H), 3.91 (s, 3H), 6.31 (d, 1H, J = 2.1 Hz), 6.50 (d, 1H, J = 2.1 Hz), 6.54 (s, 1H), 6.93 (d, 2H, J = 8.7 Hz) and 7.75 (d, 2H, J = 8.7 Hz); ^{13}C NMR ($CDCl_3$) δ 55.67, 55.96, 56.61, 92.99, 96.24, 107.76, 109.32, 114.51, 123.92, 127.75, 159.97, 160.82, 160.99, 162.21, 164.07 and 177.84.

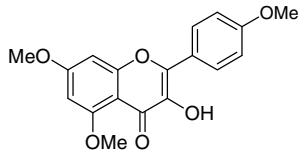

4.2.10. 4′,5,7-Tri-*O*-methylkaempferol (14).[41] To a solution containing 0.30 g (0.96 mmol) of **13** in 30 mL of CH_2Cl_2 at 0 °C was added 30 mL of a 0.9–0.11 M solution of dimethyl dioxirane (DMDO) in acetone. The reaction mixture was allowed to stir at 4 °C under N_2 overnight. The solvent was concentrated under diminished pressure and the residue was then dissolved in 50 mL of $CHCl_3$. Catalytic *p*-TsOH was added and the reaction mixture was stirred at 0 °C for 30 min. The solvent was concentrated under diminished pressure, and the resulting residue was purified by flash chromatography on a silica gel column (25 × 3 cm). Elution with 2% MeOH in $CHCl_3$ gave **14** as a light brown solid: yield 0.16 g along with 0.09 g of unreacted **13** (63% based on consumed starting material); silica gel TLC R_f 0.42 (2% MeOH in $CHCl_3$); ^{1}H NMR ($CDCl_3$) δ 3.86 (s, 3H), 3.90 (s, 3H), 3.97 (s, 3H), 6.33 (d, 1H, J = 2.1 Hz), 6.54 (d, 1H, J = 2.1 Hz), 7.02 (d, 2H, J = 8.6 Hz) and 8.16 (d, 2H, J = 8.7 Hz); ^{13}C NMR ($CDCl_3$) δ 55.3, 55.7, 56.3, 92.3, 95.6, 106.1, 113.9, 123.5, 128.8, 137.4, 142.2, 158.8, 160.4, 164.2 and 171.8.

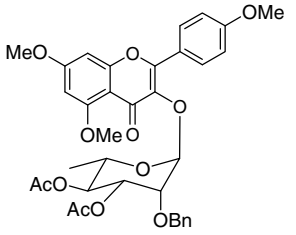

4.2.11. 4′,5,7-Tri-*O*-methylkaempferol 3-*O*-(2″-*O*-benzyl-3″,4″-di-*O*-acetyl-α-L-rhamnopyranoside) (15). To a stirred suspension containing 0.10 g (0.31 mmol) of **14**, 0.14 g (0.61 mmol) of Ag_2O, and 4 Å molecular sieves in 5 mL of CH_2Cl_2 was added 0.25 g (0.61 mmol) of **9**[13] as a solution in 5 mL of CH_2Cl_2. The reaction mixture was stirred at room temperature for 4 h, then diluted with 20 mL of CH_2Cl_2 and filtered through a Celite® pad. The filtrate was concentrated under diminished pressure and the residue was purified by flash chromatography on a silica gel column (25 × 3 cm). Elution with 2% MeOH in $CHCl_3$ gave **15** as a colorless solid: yield 0.09 g (43%); silica gel TLC R_f 0.58 (5% MeOH in $CHCl_3$); $[\alpha]_D^{22}$ −64.0 (*c* 0.3, $CHCl_3$); ^{1}H NMR ($CDCl_3$) δ 0.82 (d, 3H, J = 6.0 Hz), 1.93 (s, 3H), 1.96 (s, 3H), 3.25 (m, 1H), 3.86 (s, 3H), 3.87 (s, 3H), 3.95 (s, 3H), 4.31 (m, 1H), 4.59 (d, 1H, J = 12.0 Hz), 4.80 (d, 1H, J = 12.0 Hz), 5.06 (t, 1H, J = 9.9 Hz), 5.23 (dd, 1H, J = 10.2 and 3.3 Hz), 5.79 (d, 1H, J = 0.9 Hz), 6.34 (d, 1H, J = 2.1 Hz), 6.47 (d, 1H, J = 2.1 Hz), 7.03 (d, 2H, J = 9.0 Hz), 7.24–7.40 (m, 5H) and 7.81 (d, 2H, J = 8.7 Hz); ^{13}C NMR ($CDCl_3$) δ 17.39, 20.99, 21.09, 55.70, 56.01, 56.71, 68.33, 70.84, 71.34, 73.06, 76.06, 92.72, 96.20, 98.41, 109.61, 114.11, 123.19, 127.77, 128.13, 128.44, 130.67, 137.37, 138.28, 154.61, 159.22, 161.22, 161.51, 164.21, 170.02, 170.41 and 173.65; mass spectrum (FAB), *m/z* 649.2288 $(M+H)^+$ ($C_{35}H_{37}O_{12}$ requires 649.2285).

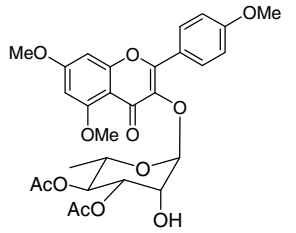

4.2.12. 4′,5,7-Tri-*O*-methylkaempferol 3-*O*-(3″,4″-di-*O*-acetyl-α-L-rhamnopyranoside) (4′,5,7-trimethoxy-SL0101) (16). A suspension containing 0.09 g (0.13 mmol) of **15** and 0.05 g of $Pd(OH)_2$/C in 6 mL of 1:1 THF–MeOH was purged with H_2 and kept under a H_2 atmosphere for 1 h. The reaction mixture was then diluted with ethyl acetate and filtered through a Celite® pad. The filtrate

was concentrated under diminished pressure to give **16** as a colorless solid: yield 0.043 g (77%); silica gel TLC R_f 0.16 (1:1:0.1 hexanes–ethyl acetate–methanol); $[\alpha]_D^{22}$ −146.6 (*c* 0.6, $CHCl_3$); ^1H NMR ($CDCl_3$) δ 0.79 (d, 3H, *J* = 6.0 Hz), 1.98 (s, 3H), 2.01 (s, 3 H), 3.32 (m, 1H), 3.88 (s, 6H), 3.94 (s, 3H), 4.17 (br s, 1H), 4.69 (br s, 1H), 5.08 (t, 1H, *J* = 9.6 Hz), 5.30 (dd, 1H, *J* = 9.6 and 3.0 Hz), 5.54 (d, 1H, *J* = 1.8 Hz), 6.31 (d, 1H, *J* = 1.5 Hz), 6.45 (d, 1H, *J* = 1.8 Hz), 7.03 (d, 2H, *J* = 8.7 Hz) and 7.84 (d, 2H, *J* = 8.7 Hz); ^{13}C NMR ($CDCl_3$) δ 17.39, 21.04, 21.18, 55.72, 56.02, 56.44, 68.19, 69.26, 71.58, 71.76, 92.58, 96.01, 101.54, 109.33, 114.06, 123.21, 130.79, 137.77, 154.96, 159.23, 161.22, 161.54, 164.38, 170.18, 170.39 and 173.75; mass spectrum (FAB), *m*/*z* 559.1813 $(M+H)^+$ ($C_{28}H_{31}O_{12}$ requires 559.1815).

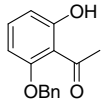

4.2.13. 2-Benzoxy-6-hydroxyacetophenone (17).[42–44] To a solution containing 10.0 g (66.0 mmol) of 2,6-dihydroxyacetophenone in 100 mL of acetone were added 13.3 g (9.2 mL, 80.0 mmol) of BnBr, 18.0 g (106 mmol) of KI, and 30.0 g (212 mmol) of K_2CO_3. The reaction mixture was heated to reflux overnight under a N_2 atmosphere, then cooled and filtered. The filtrate was concentrated under diminished pressure, then the residue was redissolved in ethyl acetate, washed with 250 mL of H_2O, dried ($MgSO_4$), and concentrated under diminished pressure. The residue was purified by flash chromatography on a silica gel column (25 × 5 cm). Elution with 2:1 hexanes–ethyl acetate gave the product **17** as a light yellow solid: yield 12.5 g (78%); mp 109–111 °C, lit.[42–44] mp 110–111 °C; silica gel TLC R_f 0.52 (3:1 hexanes–ethyl acetate); ^1H NMR ($CDCl_3$) δ 2.62 (s, 3H), 5.13 (s, 2H), 6.46 (d, 1H, *J* = 8.4 Hz), 6.59 (d, 1H, *J* = 8.4 Hz), 7.37 (m, 6H) and 13.29 (s, 1H); ^{13}C NMR ($CDCl_3$) δ 34.31, 71.34, 102.45, 111.20, 128.18, 128.68, 128.98, 135.99, 136.30, 160.84, 164.94 and 205.39.

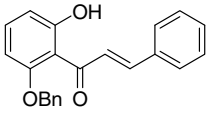

4.2.14. *E*-3-Phenyl-1-(2-benzoxy-6-hydroxyphenyl)propenone (18).[45] To a suspension containing 3.0 g (12.3 mmol) of **17** and 1.31 g (1.26 mL, 12.4 mmol) of benzaldehyde in 50 mL of MeOH was added 50 mL of 40% w/v KOH in MeOH. The reaction mixture was then heated to reflux overnight, and the cooled reaction mixture was diluted with 300 mL of water. The aqueous layer was then extracted with three 100-mL portions of ethyl acetate, washed with 75 mL of 1 N HCl, dried ($MgSO_4$), and concentrated under diminished pressure. Purification by flash chromatography on a silica gel column (25 × 4 cm), elution with 4:1 hexanes–ethyl acetate, gave **18** as an orange-yellow solid: yield 2.95 g (72%); mp 128–130 °C, lit.[45] mp 130–131 °C; silica gel TLC R_f 0.51 (3:1 hexanes–ethyl acetate); ^1H NMR ($CDCl_3$) δ 5.11 (s, 2H), 6.53 (dd, 1H, *J* = 8.4 and 0.6 Hz), 6.65 (dd, 1H, *J* = 8.4 and 0.9 Hz), 7.10 (m, 2H), 7.21 (m, 2H), 7.38–7.42 (m, 5H), 7.49 (m, 2H), 7.74 (m, 1H), 7.86 (m, 1H) and 13.57 (s, 1H); ^{13}C NMR ($CDCl_3$) δ 71.64, 102.51, 111.60, 127.88, 128.74, 128.78, 128.84, 128.93, 129.15, 130.33, 135.28, 135.82, 136.32, 143.61, 160.51, 165.76 and 194.73.

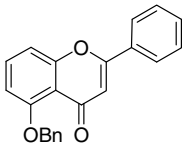

4.2.15. 5-(Benzoxy)-2-phenyl-4*H*-chromen-4-one (19).[46] To a solution containing 1.0 g (3.03 mmol) of **18** in 25 mL of DMSO was added 0.09 g (0.35 mmol) of I_2. The reaction mixture was heated to 140 °C and stirred at this temperature for 1 h. The cooled reaction mixture was then poured into 150 mL of 1 N HCl and extracted with three 100-mL portions of ethyl acetate. The combined organic layer was washed with 200 mL of brine, dried ($MgSO_4$), and concentrated under diminished pressure. The resulting residue was then purified by flash chromatography on a silica gel column (20 × 4 cm). Elution with 2:1 hexanes–ethyl acetate gave **19** as an off-white solid: yield 0.75 g (75%); mp 146–148 °C; silica gel TLC R_f 0.22 (3:1 hexanes–ethyl acetate); ^1H NMR ($CDCl_3$) δ 5.27 (s, 2H), 6.71 (s, 1H), 6.81 (d, 1H, *J* = 8.4 Hz), 7.10 (d, 1H, *J* = 8.4 Hz), 7.23–7.51 (m, 7H), 7.60 (d, 2H, *J* = 7.2 Hz) and 7.86 (m, 2H); ^{13}C NMR ($CDCl_3$) δ 71.64, 76.88, 102.51, 111.60, 127.88, 128.74, 128.78, 128.84, 128.93, 129.12, 130.33, 135.28, 135.82, 136.32, 143.61, 160.51,165.76 and 194.72; mass spectrum (FAB), *m*/*z* 329.1177 $(M+H)^+$ ($C_{22}H_{17}O_3$ requires 329.1178).

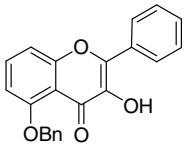

4.2.16. 5-*O*-Benzyl-4′,7-dideoxykaempferol (20). To a solution containing 0.35 g (1.1 mmol) of **19** in 20 mL of CH_2Cl_2 at 0 °C was added 20 mL of a 0.5–0.9 M solution of DMDO in acetone. The reaction mixture was stirred at 4 °C overnight, then concentrated under diminished pressure. The residue was then dissolved in 20 mL of $CHCl_3$ and cat. *p*-TsOH was added. The reaction mixture was stirred at 0 °C for 30 min and then concentrated under diminished pressure. The residue was purified by flash chromatography on a silica gel column (20 × 4 cm). Elution with 1:1 hexanes–ethyl acetate gave **20** as a light brown solid: yield 0.29 g (78%); silica gel TLC R_f 0.46 (2:1 hexanes–ethyl acetate); ^1H NMR ($CDCl_3$) δ 5.29 (s,

2H), 6.80 (d, 1H, J = 8.1 Hz), 7.13 (d, 1H, J = 8.4 Hz), 7.29–7.54 (m, 8H), 7.62 (d, 2H, J = 7.2 Hz) and 8.23 (d, 2H, J = 7.2 Hz); ^{13}C NMR ($CDCl_3$) δ 71.04, 106.89, 110.84, 112.11, 126.92, 127.70, 128.07, 128.82, 128.92, 130.13, 131.26, 134.07, 136.59, 139.00, 142.66, 157.57, 158.62 and 173.05; mass spectrum (FAB), m/z 345.1126 $(M+H)^+$ ($C_{22}H_{17}O_4$ requires 345.1127).

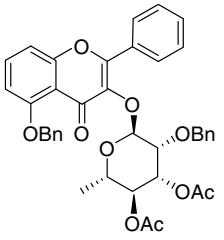

4.2.17. 5-*O*-Benzyl-4′,7-dideoxykaempferol 3-*O*-(2″-*O*-benzyl-3″,4″-di-*O*-acetyl-α-L-rhamnopyranoside) (21). To a stirred suspension containing 0.10 g (0.29 mmol) of **20**, 0.14 g (0.58 mmol) of Ag_2O, and 4Å molecular sieves in 5 mL of CH_2Cl_2 was added 0.23 g (0.58 mmol) of **9**[13] as a solution in 3 mL of CH_2Cl_2. The reaction mixture was stirred at room temperature for 4 h, then diluted with 20 mL of CH_2Cl_2 and filtered through a Celite® pad. The filtrate was concentrated under diminished pressure and purified by flash chromatography on a silica gel column (25 × 3 cm). Elution with 3:1 hexanes–ethyl acetate gave **21** as a colorless foam: yield 0.17 g (86%); silica gel TLC R_f 0.26 (2:1 hexanes–ethyl acetate); $[\alpha]_D^{22}$ −89.5 (c 1.0, $CHCl_3$); ^{1}H NMR ($CDCl_3$) δ 0.80 (d, 3H, J = 6.3 Hz), 1.92 (s, 3H), 1.97 (s, 3H), 3.29 (m, 1H), 4.38 (m, 1H), 4.63 (d, 1H, J = 12.3 Hz), 4.78 (d, 1H, J = 12.3 Hz), 5.08 (t, 1H, J = 9.9 Hz), 5.22 (dd, 1H, J = 10.2 and 3.3 Hz), 5.30 (d, 2H), 5.70 (d, 1H, J = 1.5 Hz), 6.80 (d, 1H, J = 8.1 Hz), 7.05 (d, 1H, J = 8.7 Hz), 7.23–7.55 (m, 12H), 7.61 (d, 2H, J = 7.5 Hz) and 7.88 (m, 2H); ^{13}C NMR ($CDCl_3$) δ 17.24, 20.98, 21.02, 68.41, 70.69, 71.06, 71.13, 72.83, 75.63, 98.89, 108.13, 110.65, 115.45, 126.83, 127.86, 128.41, 128.44, 128.64, 128.73, 129.13, 130.72, 130.85, 133.83, 136.69, 138.11, 138.51, 155.03, 157.64, 158.91, 170.00, 170.30 and 174.08; mass spectrum (FAB), m/z 665.2389 $(M+H)^+$ ($C_{39}H_{37}O_{10}$ requires 665.2387).

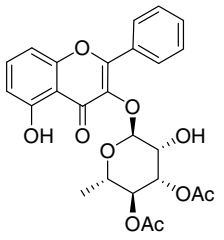

4.2.18. 4′,7-Dideoxykaempferol 3-*O*-(3″,4″-di-*O*-acetyl-α-L-rhamnopyranoside (4′,7-dideoxy-SL0101)) (22). A suspension containing 0.11 g (0.17 mmol) of **21** and 0.03 g of $Pd(OH)_2$/C in 6 mL of 1:1 THF–MeOH was purged three times with H_2. The reaction vessel was then maintained under a H_2 atmosphere for 1 h, then filtered through a Celite® pad and washed with ethyl acetate. The filtrate was concentrated under diminished pressure to afford a solid. The product **22** was pure enough so that further purification was unnecessary: yield 0.08 g (95%); silica gel TLC R_f 0.62 (1:1:0.1 hexanes–ethyl acetate–methanol); $[\alpha]_D^{21}$ −143.2 (c 0.9, $CHCl_3$); ^{1}H NMR ($CDCl_3$) δ 0.80 (d, 3H, J = 6.5 Hz), 1.98 (s, 3H), 2.08 (s, 3H), 3.13 (br s, 1H), 3.32 (m, 1H), 4.48 (s, 1H), 5.00 (t, 1H, J = 9.5 Hz), 5.22 (dd, 1H, J = 9.5 and 3.0 Hz), 5.52 (d, 1H, J = 1.0 Hz), 6.77 (d, 1H, J = 8.0 Hz), 6.94 (d, 1H, J = 8.5 Hz), 5.55 (m, 4H), 7.90 (m, 2H) and 12.23 (s, 1H); ^{13}C NMR ($CDCl_3$) δ 17.23, 20.96, 21.15, 68.44, 69.28, 71.03, 71.40, 101.18, 107.42, 111.10, 111.41, 128.87, 129.24, 130.36, 131.43, 135.73, 136.12, 155.83, 158.55, 160.86, 170.26, 170.37 and 179.50; mass spectrum (FAB), m/z 485.1450 $(M+H)^+$ ($C_{25}H_{25}O_{10}$ requires 485.1448).

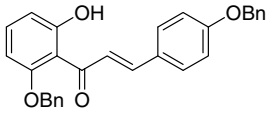

4.2.19. *E*-3-(4-Benzoxyphenyl)-1-(2-benzoxy-6-hydroxyphenyl)propenone (23). To a solution containing 2.00 g (8.26 mmol) of **17** and 1.93 g (9.10 mmol) of 4-(benzoxy)benzaldehyde in 50 mL of MeOH was added 50 mL of 40% w/v KOH in MeOH. The reaction mixture was heated to reflux overnight, cooled to room temperature, and poured into 300 mL of H_2O. The aqueous layer was extracted with three 100-mL portions of ethyl acetate. The combined organic layer was dried ($MgSO_4$) and concentrated under diminished pressure. The residue was purified by flash chromatography on a silica gel column (24 × 4 cm). Elution with 3:1 hexanes–ethyl acetate gave **23** as a bright yellow solid: yield 2.70 g (75%); mp 120–122 °C; silica gel TLC R_f 0.39 (6:1 hexanes–ethyl acetate); ^{1}H NMR ($CDCl_3$) δ 5.08 (s, 4H), 6.51 (d, 1H, J = 8.1 Hz), 6.65 (d, 1H, J = 8.1 Hz), 6.79 (d, 2H, J = 8.7 Hz), 7.03 (d, 2H, J = 8.7 Hz), 7.33–7.51 (m, 11H), 7.77 (m, 2H), and 13.78 (s, 1H); ^{13}C NMR ($CDCl_3$) δ 70.22, 71.53, 102.40, 111.51, 111.91, 115.22, 125.57, 127.68, 128.27, 128.39, 128.70, 128.85, 128.89, 129.09, 130.53, 135.86, 136.02, 136.67, 143.61, 160.41, 160.67, 165.79 and 194.46; mass spectrum (FAB), m/z 437.1754 $(M+H)^+$ ($C_{29}H_{25}O_4$ requires 437.1753).

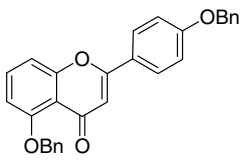

4.2.20. 5-(Benzoxy)-2-(4-(benzoxy)phenyl)-4*H*-chromen-4-one (24). To a solution containing 1.00 g (2.29 mmol) of **23** in 20 mL of DMSO at 140 °C was added 0.06 g

(0.23 mmol) of I_2. The reaction mixture was stirred at 140 °C for 30 min, then cooled to room temperature and poured into 200 mL of H_2O. The aqueous layer was extracted with three 75-mL portions of ethyl acetate. The combined organic layer was washed with 200 mL of brine, dried ($MgSO_4$), and concentrated under diminished pressure. The residue was purified by flash chromatography on a silica gel column (20 × 4 cm). Elution with 2:1 hexanes–ethyl acetate gave **24** as a colorless foam: yield 0.76 g (76%); mp 145–147 °C; silica gel TLC R_f 0.10 (3:1 hexanes–ethyl acetate); ^{1}H NMR ($CDCl_3$) δ 5.12 (s, 2H), 5.28 (s, 2H), 6.81 (s, 1H), 6.82 (d, 1H, J = 8.1 Hz), 7.06 (d, 2H, J = 8.7 Hz), 7.08 (d, 1H, J = 8.1 Hz), 7.40 (m, 9H), 7.64 (d, 2H, J = 7.5 Hz) and 7.82 (d, 2H, J = 8.7 Hz); ^{13}C NMR ($CDCl_3$) δ 70.32, 71.02, 107.98, 108.62, 110.62, 115.43, 124.13, 126.79, 127.67, 127.80, 127.96, 128.43, 128.76, 128.90, 133.61, 136.44, 136.85, 158.40, 158.67, 161.20, 161.49 and 178.24; mass spectrum (FAB), *m/z* 435.1598 $(M+H)^+$ ($C_{29}H_{23}O_4$ requires 435.1597).

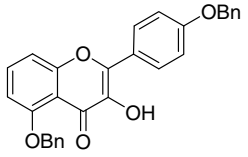

4.2.21. 7-Deoxy-4′,5-di-*O*-benzylkaempferol (25). To a solution containing 0.30 g (0.69 mmol) of **24** in 20 mL of CH_2Cl_2 at 0 °C was added 20 mL of a 0.5–0.9 M solution of DMDO in acetone. The reaction mixture was stirred at 4 °C overnight and then concentrated under diminished pressure. The residue was then dissolved in 20 mL of $CHCl_3$ and cat. *p*-TsOH was added. The reaction mixture was stirred at 0 °C for 30 min and concentrated under diminished pressure. The residue was purified by flash chromatography on a silica gel column (26 × 3 cm). Elution with 3:1 hexanes–ethyl acetate gave **25** as a light brown solid: yield 0.22 g (72%); silica gel TLC R_f 0.26 (3:1 hexanes–ethyl acetate); ^{1}H NMR ($CDCl_3$) δ 5.14 (s, 2H), 5.29 (s, 2H), 7.10 (d, 2H, J = 8.4 Hz), 7.35–7.52 (m, 11H), 7.65 (d, 2H, J = 7.5 Hz) and 8.20 (d, 2H, J = 8.4 Hz); ^{13}C NMR ($CDCl_3$) δ 70.25, 70.99, 106.86, 110.75, 112.10, 115.13, 123.91, 126.89, 127.71, 128.01, 128.36, 128.88, 129.40, 133.75, 136.64, 136.71, 138.18, 142.98, 157.37, 158.51, 160.18 and 172.74; mass spectrum (FAB), *m/z* 451.1544 $(M+H)^+$ ($C_{29}H_{23}O_5$ requires 451.1546).

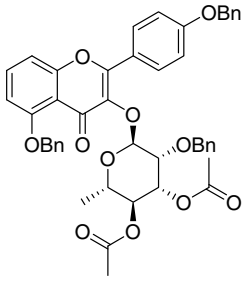

4.2.22. 7-Deoxy-4′,5-di-*O*-benzylkaempferol 3-*O*-(2″-*O*-Benzyl-3″,4″-di-*O*-acetyl-α-L-rhamnopyranoside) (26). To a stirred suspension containing 0.11 g (0.24 mmol) of **25**, 0.11 g (0.49 mmol) of Ag_2O, and 4Å molecular sieves in 10 mL of CH_2Cl_2 was added 0.20 g (0.49 mmol) of **9**[13] as a solution in 3 mL of CH_2Cl_2. The reaction mixture was stirred at room temperature for 4 h, then diluted with 20 mL of CH_2Cl_2 and filtered through a Celite® pad. The filtrate was concentrated under diminished pressure and purified by flash chromatography on a silica gel column (20 × 3 cm). Elution with 3:1 hexanes–ethyl acetate gave **26** as a colorless foam: yield 0.13 g (67%); silica gel TLC R_f0.17 (2:1 hexanes–ethyl acetate); $[\alpha]_D^{21}$ −86.5 (*c* 0.9, $CHCl_3$); ^{1}H NMR ($CDCl_3$) δ 0.87 (d, 3H, J = 6.3 Hz), 1.95 (s, 3H), 1.99 (s, 3H), 3.44 (m, 1H), 4.39 (dd, 1H, J = 3.3 and 1.8 Hz), 4.70 (d, 1H, J = 12.3 Hz), 4.83 (d, 1H, J = 12.3 Hz), 5.10 (d, 1H, J = 9.9 Hz), 5.15 (s, 2H), 5.28 (dd, 1H, J = 10.2 and 3.3 Hz), 5.32 (s, 2H), 5.73 (d, 1H, J = 1.5 Hz), 6.81 (d, 1H, J = 8.1 Hz), 7.28–7.48 (m, 17H), 7.64 (d, 2H, J = 7.2 Hz) and 7.86 (d, 2H, J = 8.7 Hz); ^{13}C NMR ($CDCl_3$) δ 17.35, 21.08, 68.47, 70.31, 70.75, 71.11, 71.31, 72.87, 75.76, 98.92, 108.15, 110.64, 114.98, 115.47, 123.37, 126.88, 127.57, 127.87, 128.41, 128.47, 128.77, 128.90, 130.79, 133.79, 136.53, 136.77, 138.12, 138.18, 154.91, 157.58, 158.92, 160.75, 170.04, 170.35 and 174.07; mass spectrum (FAB), *m/z* 771.2808 $(M+H)^+$ ($C_{46}H_{43}O_{11}$ requires 771.2805).

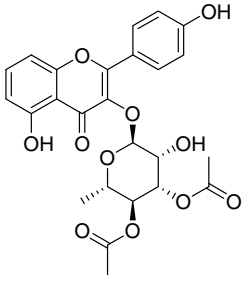

4.2.23. 7-Deoxykaempferol 3-*O*-(3″,4″-di-*O*-acetyl-α-L-rhamnopyranoside) (7-deoxy-SL0101) (27). A suspension containing 0.30 g (0.39 mmol) of **26** and 0.07 g of $Pd(OH)_2$/C in 6 mL of 1:1 THF–MeOH was purged three times with H_2. The reaction vessel was then kept under a H_2 atmosphere for 1 h, filtered through a Celite® pad, and washed with ethyl acetate. The filtrate was concentrated under diminished pressure to afford a solid. Product **27** was pure and further purification was not necessary: yield 0.17 g (86%); silica gel TLC R_f 0.43 (1:1:0.1 hexanes–ethyl acetate–methanol); $[\alpha]_D^{21}$ −103.3 (*c* 0.8, MeOH); ^{1}H NMR (acetone-d_6) δ 0.83 (d, 3H, J = 6.0 Hz), 1.97 (s, 3H), 2.03 (s, 3H), 3.00 (br s, 1H), 3.55 (m, 1H), 4.46 (m, 1H), 4.82 (br s, 1H), 5.09 (t, 1H, J = 9.6 Hz), 5.22 (d, 1H, J = 9.3 Hz), 5.59 (s, 1H), 6.77 (d, 1H, J = 7.8 Hz), 7.07 (d, 2H, J = 7.8 Hz), 7.65 (t, 1H, J = 7.8 Hz), 7.92 (d, 2H, J = 7.2 Hz), 9.26 (br s, 1H) and 12.48 (s, 1H); ^{13}C NMR (acetone-d_6) δ 17.35, 21.05, 21.25, 68.52, 69.35, 71.32, 71.72, 100.99, 107.47, 111.10, 111.31, 116.07, 122.00, 131.17, 135.26, 135.63,

155.72, 158.87, 159.50, 160.77, 170.82, 171.09 and 179.43; mass spectrum (FAB), *m/z* 501.1395 $(M+H)^+$ ($C_{25}H_{25}O_{11}$ requires 501.1397).

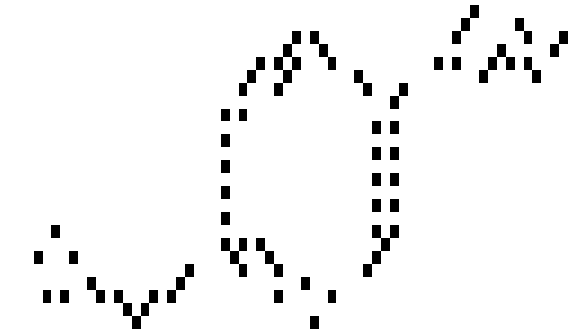

4.2.24. 4′,5,7-Tri-*O*-acetylkaempferol 3-*O*-(2″,3″,4″-tri-*O*-acetyl-α-L-rhamnopyranoside) (Peracetylated-SL0101) (28). To a solution containing 0.038 g (0.068 mmol) of kaempferol 3-*O*-(2″,3″,4″-triacetoxy-α-L-rhamnopyranoside) (**29**)[18] in 4 mL of CH_2Cl_2 were added 0.035 g (0.034 mmol, 0.03 mL) of acetic anhydride, 0.048 g (0.48 mmol, 0.07 mL) of triethylamine, and cat. DMAP. The reaction mixture was stirred at room temperature under N_2 for 4 h, then quenched with 15 mL of brine and extracted with three 15-mL portions of ethyl acetate. The combined organic layer was dried ($MgSO_4$) and concentrated under diminished pressure. Purification by flash chromatography on a silica gel column (2 × 30 cm) using 1:1 ethyl acetate–hexanes gave **28** as a colorless oil: yield 0.044 g (95%); ^{1}H NMR ($CDCl_3$) δ 0.85 (d, 3H, J = 6.3 Hz), 1.96 (s, 3H), 1.97 (s, 3H), 2.11 (s, 3H), 2.31 (s, 3H), 2.33 (s, 3H), 2.43 (s, 3H), 3.24 (m, 1H), 4.91 (t, 1H, J = 9.9 Hz), 5.25 (dd, 1H, J = 10.2 and 3.3 Hz), 5.56 (d, 1H, J = 1.5 Hz), 5.63 (m, 1H), 6.82 (d, 1H, J = 2.4 Hz), 7.27 (m, 3H) and 7.89 (d, 2H, J = 8.7 Hz); ^{13}C NMR ($CDCl_3$) δ 16.95, 20.62, 20.69, 20.85, 21.05, 21.08, 21.13, 68.37, 68.77, 69.04, 70.23, 93.01, 108.92, 113.56, 115.11, 122.17, 127.42, 130.13, 136.94, 150.32, 152.70, 153.90, 155.25, 156.64, 156.68, 157.96, 168.65, 169.37, 169.60, 169.91, 169.98 and 172.21; mass spectrum (FAB), *m/z* 685.1766 $(M+H)^+$ ($C_{33}H_{33}O_{16}$ requires 685.1769).

4.3. Kinase assays

Glutathione-*S*-transferase (GST)-fusion protein (1 μg) containing the sequence—RRRLASTNDKG (for serine/threonine kinase assays) was adsorbed in the wells of LumiNunc 96-well polystyrene plates (MaxiSorp surface treatment). The wells were blocked with sterile 3% tryptone in phosphate-buffered saline. Kinase (5 nM) in 70 μL of kinase buffer (5 mM β-glycerophosphate, pH 7.4, 25 mM HEPES, pH 7.4, 1.5 mM DTT, 30 mM $MgCl_2$, 0.15 M NaCl) was dispensed into each well. Compound at the indicated concentrations or vehicle was added and reactions were initiated by the addition of 30 μL of ATP to a final ATP concentration of 10 μM. Reactions were terminated after 30 min by addition of 75 μL of 500 mM EDTA, pH 7.5. All assays measured the initial velocity of reaction. After extensive washing of wells, anti-p-p140 antibody, a polyclonal phosphospecific antibody developed against the phosphopeptide, CGLASTND, and HRP-conjugated anti-rabbit antibody (211-035-109, Jackson ImmunoResearch Laboratories, West Grove, Pennsylvania) were used to detect serine phosphorylation of the substrate. HRP activity was measured using Western Lightning Chemiluminescence Reagent (NEL102, PerkinElmer Life Sciences) according to the manufacturer's protocol. Maximum and minimum activity is the relative luminescence detected in the presence of vehicle and 200 mM EDTA, respectively. His-tagged active RSK was expressed in Sf9 cells and purified using NiNTA resin (Qiagen, Valencia, California). Baculovirus was prepared using the Bac-to-Bac® baculovirus expression system (Invitrogen, Carlsbad, California). Maximum responses and the concentrations at half the inhibitory response (IC_{50}) were determined by performing a best-fit analysis of the data (GraphPad Prism).

4.4. Cell culture

For proliferation studies cells were seeded at 5000 cells per well in 96-well tissue culture plates in the appropriate medium as described by American Type Culture Collection. After 24 h, the medium was replaced with medium containing compound or vehicle as indicated. Cell viability was measured 48 h later using CellTiter-Glo™ assay reagent (Promega, Madison, Wisconsin) according to the manufacturer's protocol. Maximum responses and the concentrations of half the effective response (EC_{50}) were determined by performing a best-fit analysis of the data (GraphPad Prism). For specificity studies, cells were seeded at 3×10^5 cells/well in 6-well plates. After 24 h, the cells were serum-starved for 24 h and then incubated with compound or vehicle for 4 h prior to a 20-min treatment with phorbol myristate acetate. Cells were lysed with boiling SDS-sample buffer without dithiothreitol (DTT). The lysates were normalized for total protein, and DTT was added to an aliquot, which was electrophoresed and immunoblotted. Antibodies used on cell lysates included anti-pan-MAPK (anti-ERK1/2) (610124) from BD Transduction Laboratories; anti-phospho-MAPK (V8031) from Promega; anti-eEF2 (2332), anti-phospho-eEF2 (2331), anti-phospho-Akt Substrate (9611), anti-phospho-PKA Substrate (9621), and anti-phospho-PKC Substrate (2261) from Cell Signaling Technology. Anti-Ran was a generous gift from Ian Macara (University of Virginia).

Acknowledgment

This work was supported by the Department of Defense #DAMD17-03-1-0366 USAMRMC. We thank Ian Macara for a sample of anti-Ran.

References and notes

1. Roux, P. P.; Blenis, J. *Microbiol. Mol. Biol. Rev.* **2004**, *68*, 320–344.

2. Smith, J. A.; Poteet-Smith, C. E.; Xu, Y.; Errington, T. M.; Hecht, S. M.; Lannigan, D. A. *Cancer Res.* **2005**, *65*, 1027–1034.
3. Clark, D. E.; Errington, T. M.; Smith, J. A.; Frierson, H. F., Jr.; Weber, M. J.; Lannigan, D. A. *Cancer Res.* **2005**, *65*, 3108–3116.
4. Hurbin, A.; Coll, J. L.; Dubrez-Daloz, L.; Mari, B.; Auberger, P.; Brambilla, C.; Favrot, M. C. *J. Biol. Chem.* **2005**, *280*, 19757–19767.
5. David, J. P.; Mehic, D.; Bakiri, L.; Schilling, A. F.; Mandic, V.; Priemel, M.; Idarraga, M. H.; Reschke, M. O.; Hoffmann, O.; Amling, M.; Wagner, E. F. *J. Clin. Invest.* **2005**, *115*, 664–672.
6. Hayashi, M.; Fearns, C.; Eliceiri, B.; Yang, Y.; Lee, J. D. *Cancer Res.* **2005**, *65*, 7699–7706.
7. Xu, Y.-M.; Smith, J. A.; Lannigan, D. A.; Hecht, S. M. *Bioorg. Med. Chem.* **2006**, *14*, 3974–3977.
8. Vieth, M.; Sutherland, J. J.; Robertson, D. H.; Campbell, R. M. *Drug Discov. Today* **2005**, *10*, 839–846.
9. Noble, M. E.; Endicott, J. A.; Johnson, L. N. *Science* **2004**, *303*, 1800–1805.
10. Nguyen, T. L.; Gussio, R.; Smith, J. A.; Lannigan, D. A.; Hecht, S. M.; Scudiero, D. A.; Shoemaker, R. H.; Zaharevitz, D. W. *Bioorg. Med. Chem.* **2006**, *14*, 6097–6105.
11. Prade, L.; Engh, R. A.; Girod, A.; Kinzel, V.; Huber, R.; Bossemeyer, D. *Structure* **1997**, *5*, 1627–1637.
12. Xu, Z. B.; Chaudhary, D.; Olland, S.; Wolfrom, S.; Czerwinski, R.; Malakian, K.; Lin, L.; Stahl, M. L.; Joseph-McCarthy, D.; Benander, C.; Fitz, L.; Greco, R.; Somers, W. S.; Mosyak, L. *J. Biol. Chem.* **2004**, *279*, 50401–50409.
13. Maloney, D. J.; Hecht, S. M. *Org. Lett.* **2005**, *7*, 1097–1099.
14. Algar, J.; Flynn, J. P. *Proc. R. Irish Acad.* **1934**, *42b*, 1–8.
15. Oyamada, T. *Nippon Kagaku Kaishi* **1934**, *55*, 1256–1261.
16. Oyamada, T. *Bull. Chem. Soc. Jpn.* **1935**, *10*, 182–186.
17. De Meyer, N.; Haemers, A.; Mishra, L.; Pandey, H. K.; Pieters, L. A. C.; Vanden Berghe, D. A.; Vlietinck, A. *J. Med. Chem.* **1992**, *34*, 736–746.
18. Smith, J. A.; Maloney, D. J.; Clark, D. E.; Xu, Y.; Hecht, S. M.; Lannigan, D. A. *Bioorg. Med. Chem.* **2006**, *14*, 6034–6042.
19. Sapkota, G. P.; Newell, F. S.; Armstrong, C.; Bain, J.; Frodin, M.; Grauert, M.; Hoffmann, M.; Schnapp, G.; Steegmaier, M.; Cohen, P.; Alessi, D. R. *Biochem. J.* **2007**, *401*, 29–38.
20. Cohen, M. S.; Zhang, C.; Shokat, K. M.; Taunton, J. *Science* **2005**, *308*, 1318–1321.
21. Takeishi, Y.; Huang, Q.; Abe, J.; Che, W.; Lee, J. D.; Kawakatsu, H.; Hoit, B. D.; Berk, B. C.; Walsh, R. A. *Cardiovasc. Res.* **2002**, *53*, 131–137.
22. McDonald, C.; Vacratsis, P. O.; Bliska, J. B.; Dixon, J. E. *J. Biol. Chem.* **2003**, *278*, 18514–18523.
23. Lu, H.; Guizzetti, M.; Costa, L. G. *J. Pharmacol. Exp. Ther.* **2002**, *300*, 818–823.
24. Zhu, X.; Castellani, R. J.; Takeda, A.; Nunomura, A.; Atwood, C. S.; Perry, G.; Smith, M. A. *Mech. Ageing Dev.* **2001**, *123*, 39–46.
25. Valjent, E.; Corvol, J. C.; Pages, C.; Besson, M. J.; Maldonado, R.; Caboche, J. *J. Neurosci.* **2000**, *20*, 8701–8709.
26. Ji, R. R.; Befort, K.; Brenner, G. J.; Woolf, C. J. *J. Neurosci.* **2002**, *22*, 478–485.
27. Kulich, S. M.; Chu, C. T. *J. Neurochem.* **2001**, *77*, 1058–1066.
28. Gomez-Santos, C.; Ferrer, I.; Reiriz, J.; Vinals, F.; Barrachina, M.; Ambrosio, S. *Brain Res.* **2002**, *935*, 32–39.
29. Hu, Y.; Dietrich, H.; Metzler, B.; Wick, G.; Xu, Q. *Arterioscler. Thromb. Vasc. Biol.* **2000**, *20*, 18–26.
30. Bokemeyer, D.; Panek, D.; Kramer, H. J.; Lindemann, M.; Kitahara, M.; Boor, P.; Kerjaschki, D.; Trzaskos, J. M.; Floege, J.; Ostendorf, T. *J. Am. Soc. Nephrol.* **2002**, *13*, 1473–1480.
31. Pahl, A.; Zhang, M.; Kuss, H.; Szelenyi, I.; Brune, K. *Br. J. Pharmacol.* **2002**, *135*, 1915–1926.
32. Slomiany, B. L.; Slomiany, A. *Biochem. Biophys. Res. Commun.* **2002**, *294*, 220–224.
33. Opavsky, M. A.; Martino, T.; Rabinovitch, M.; Penninger, J.; Richardson, C.; Petric, M.; Trinidad, C.; Butcher, L.; Chan, J.; Liu, P. P. *J. Clin. Invest.* **2002**, *109*, 1561–1569.
34. Planz, O.; Pleschka, S.; Ludwig, S. *J. Virol.* **2001**, *75*, 4871–4877.
35. Dineley, K. T.; Westerman, M.; Bui, D.; Bell, K.; Ashe, K. H.; Sweatt, J. D. *J. Neurosci.* **2001**, *21*, 4125–4133.
36. Delaunoy, J. P.; Dubos, A.; Marques Pereira, P.; Hanauer, A. *Clin. Genet.* **2006**, *70*, 161–166.
37. Dufresne, S. D.; Bjorbaek, C.; El-Haschimi, K.; Xhao, Y.; Aschenbach, W. G.; Moller, D. E.; Goodyear, L. J. *Mol. Cell. Biol.* **2001**, *8*, 81–87.
38. Kim, M.; Lee, J. H.; Koh, H.; Lee, S. Y.; Jang, C.; Chung, C. J.; Sung, J. H.; Blenis, J.; Chung, J. *EMBO J.* **2006**, *25*, 3056–3067.
39. Geissman, T. A.; Clinton, R. O. *J. Am. Chem. Soc.* **1946**, *68*, 697–700.
40. Machida, K.; Osawa, K. *Chem. Pharm. Bull.* **1989**, *37*, 1092–1094.
41. Jain, N.; Alam, M. S.; Kamil, M.; Ilyas, M.; Niwa, M.; Sakae, A. *Phytochemistry* **1990**, *29*, 3988–3991.
42. Murata, T.; Shimada, M.; Sakakibera, S.; Yoshino, T.; Masuda, T.; Shintani, T.; Sato, H.; Koriyama, Y.; Fukushima, K.; Nunami, N.; Yamauchi, M. *Bioorg. Med. Chem. Lett.* **2004**, *14*, 4019–4022.
43. Pinto, D. G.; Silva, A. M. S.; Cavaleiro, J. A. *J. Heterocycl. Chem.* **2000**, *37*, 1629–1634.
44. Patil, A. D.; Deshpande, V. H. *Indian J. Chem. Sect. B* **1983**, *22*, 109–113.
45. Pinto, D. G.; Silva, A. M. S.; Cavaleiro, J. A. *J. Heterocycl. Chem.* **1996**, 1887–1893.
46. Pinto, D. G.; Silva, A. M. S.; Cavaleiro, J. A. *Tetrahedron Lett.* **1994**, *35*, 5899–5902.